PHYSICAL REVIEW C VOLUME 6, NUMBER 2 AUGUST 1972

Nuclear Levels in ^{188}Re†

E. B. Shera
University of California, Los Alamos Scientific Laboratory, Los Alamos, New Mexico 87544

and

U. Gruber, B. P. K. Maier, H. R. Koch, and O. W. B. Schult
Technical University, Munich, Germany,
and Research Establishment of The Danish Atomic Energy Commission, Risø, Roskilde, Denmark

and

R. G. Lanier
University of California, Lawrence Livermore Laboratory, Livermore, California 94550

and

N. Onishi and R. K. Sheline
Florida State University, Tallahassee, Florida 32304
(Received 24 April 1972)

Nuclear levels in ^{188}Re have been investigated using the following experimental techniques: measurement of neutron-capture γ-ray transitions with energies between 4.8 and 6.0 MeV using a Ge(Li) pair spectrometer; study of (d,p) spectra using 12-MeV deuterons and a broad-range magnetic spectrograph; measurement of (n,γ) spectra between 45 and 830 keV with a bent-crystal spectrometer; coincidence studies of the (n,γ) radiation using two Ge(Li) detectors, including a study of short-lived isomeric states using delayed-coincidence techniques; and observation of the γ rays following β decay of ^{188}W using a Ge(Li) detector. A nuclear level scheme for ^{188}Re has been constructed by combining the results of the above measurements with published data. Information, including spin and parity assignments, is presented on 36 low-lying levels. The lifetimes of five excited states are reported. The Nilsson model has been used to interpret the level structure. Assignments are proposed which involve 15 separate rotational bands. Proposed Nilsson configurations, band-head energies, and band-head lifetimes (if known) are: $1^-[402\uparrow-512\downarrow]$, 0.0 keV; $3^-[402\uparrow+510\uparrow]$, 169.4 keV; $6^-[402\uparrow+503\uparrow]$, 172.1 keV, 19 min; $4^-[402\uparrow+512\downarrow]$, 182.7 keV, 18 nsec; $2^-[402\uparrow-505\downarrow]$, 205.3 keV, 3.2 nsec; $0^+[514\uparrow-505\downarrow]$, 207.9 keV, 3.2 nsec; $3^+[514\uparrow-512\downarrow]$, 230.9 keV, 21 nsec; $2^-[402\uparrow-510\uparrow]$, 256.9 keV; $1^-[402\uparrow+503\uparrow]$, 290.7 keV; $4^-[402\uparrow+501\uparrow]$, 325.9 keV; $5^+[514\uparrow+510\uparrow]$, 360.9 keV, 5.2 nsec; $3^+[402\uparrow-615\uparrow]$, 439.7 keV; $1^+[514\uparrow-503\uparrow]$, 482.2 keV; $1^-[402\uparrow-501\uparrow]$, 556.8 keV. A $K^\pi=1^-$ band, believed to be predominantly a $|K-2|$ γ-vibrational band, is observed at 582.2 keV. The measured (d,p) reaction cross sections are compared with theoretical calculations based on these assignments. The β-decay measurements have revealed a previously unknown β branch from the ^{188}W ground state to a $I^\pi=0^+$ level at 207.9 keV. This $0^+\to0^+$ transition ($\log ft=9.9$) is discussed in terms of isobaric analog state mixing. Results of a calculation which uses a parametrized residual neutron-proton interaction to predict the parallel-antiparallel splitting energies and $K=0$ even-odd shifts in ^{186}Re and ^{188}Re are presented and compared with experiment.

I. INTRODUCTION

The nucleus ^{188}Re lies at the upper end of a mass region which is between the strongly deformed nuclei of lower mass and the spherical nuclei of the Pb region. Interest in this mass region has stimulated several previous investigations of this odd-odd nucleus. The first comprehensive study of the ^{188}Re structure was reported by Burson *et al.*,[1] who investigated the radioactive decay of ^{188}W and the ^{188}Re isomer. The 18.5-min isomer has also been extensively studied by Takahashi, McKeown, and Scharff-Goldhaber.[2] Recently, several investigations of the γ rays[3,4] and the internal-conversion electron spectra[5,6] following neutron capture have also been reported. The internal-conversion and multipolarity data of Suarez *et al.*[6] were of particular value to the present investigation since these data are often crucial in establishing level spins and parities.

The level scheme of Fig. 1, which is derived primarily from the work of Burson *et al.*[1] and Suarez *et al.*,[6] is used to summarize what has been reasonably well established by previous investigations of ^{188}Re. The previous theoretical interpretation of this level structure, based on the deformed model, is also indicated in Fig. 1.

II. EXPERIMENTAL RESULTS

A. High-Energy (n, γ) Spectrum

The high-energy neutron-capture γ-ray spectrum was measured with a lithium-drifted germanium spectrometer at Los Alamos. A typical spectrum is shown in Fig. 2. Details of the spectrometer, which employs an annular NaI detector to suppress all but pair peaks in the recorded spectrum, are given in the work of Jurney, Motz, and Vegors.[7] The spectrometer calibration was performed using as standards the energies[8] and cross sections[9] of the nitrogen lines emitted from a melamine target. The effect of electronic nonlinearity on the energy calibration of the spectrometer was corrected by using the sliding pulser technique recently developed by Strauss, Lenkszus, and Eichholz.[10]

The ^{187}Re target used in these measurements was obtained from Oak Ridge National Laboratory and consisted of 163 mg of rhenium metal enriched to 99.22% in ^{187}Re. The thermal-neutron cross sections of ^{185}Re and ^{187}Re are, respectively, 105 and 73 b,[11] and hence in the above target 99.0% of the total capture occurred in ^{187}Re. The data from a separate study[12] of an enriched ^{185}Re target have been used to correct the present data for the small contamination from this isotope.

The measured γ-ray energies and intensities from the reaction $^{187}\mathrm{Re}(n, \gamma)^{188}\mathrm{Re}$ are listed in Table I. The ground-state spin and parity assignment of ^{187}Re is $\frac{5}{2}^+$ and the assignment of the compound state formed after thermal-neutron capture is therefore 2^+ or 3^+. Assuming, as is overwhelmingly the case, that only $E1$ and $M1$ transitions occur from the capture state to lower levels, transitions are permitted only to states with spins and parities $1^\pm$ to $4^\pm$. The more energetic of the observed transitions, the energies of which differ from the binding energy by less than 2 MeV, are assumed to correspond to primary transitions from the capture state directly to a low-lying level.

The neutron binding energy in ^{188}Re has been determined to be 5871.6 ± 0.3 keV by observation of the intense primary transition to the ground state. This value of the binding energy has been used to

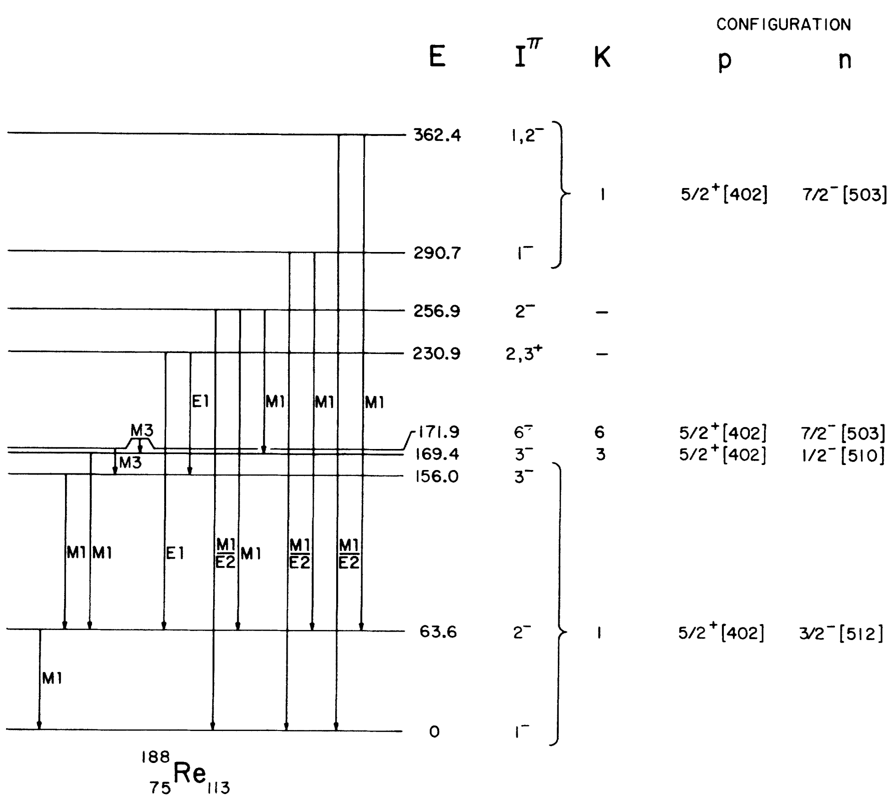

FIG. 1. ^{188}Re level scheme summarizing previous work; it is derived principally from Burson *et al.* (Ref. 1) and Suarez *et al.* (Ref. 6).

calculate the excitation energy of the excited states of ^{188}Re listed in Table I. A minimum error of ±0.3 keV has been assigned to all of the primary γ-ray energies since these values include the uncertainty in the ^{15}N neutron binding energy upon which the energy calibration is based. The excitation energies, which involve only energy differences, are assigned smaller errors.

B. Low-Energy (n, γ) Spectrum

The high-resolution study of the low-energy ^{187}Re(n, γ) spectrum has been performed with the curved-crystal diffractometer at Risø. The instrument has been described previously.[13] Also the method of data collection and analysis has been given in detail.[14] The source consisted of about 50 mg of ^{187}Re metal enriched[15] to 98.8%. The γ spectrum was recorded in the range from 25 keV to 1.2 MeV. During this measurement, the full energy width at half maximum, ΔE, of a γ line with energy E was

$$\Delta E/E \approx (9\times10^{-6})E(\mathrm{keV})/n\ ,$$

where n is the order of reflection. For strong lines, $n=1$–5; for transitions of intermediate intensity, $n=1$–3; and for weak lines, $n=1$–2. γ-ray transitions below 50 keV were only recorded in the first order of reflection. The energy calibration of the spectrometer was performed with the use of the $K\alpha_1$ and $K\alpha_2$ lines of Re, which have been measured precisely by Bergvall.[16] Absolute transition intensities were obtained with reference to the 155-keV γ line emitted after the β decay of ^{188}Re. Several γ transitions which were due to the ^{185}Re(n, γ) reaction were identified through a separate run taken for the study of the low-energy (n, γ) lines of ^{186}Re.[12] The results of this investigation of the low-energy capture γ-ray spectrum of ^{188}Re are listed in Table II. The internal-conversion-electron results of Suarez *et al.*[6] are also included in this table.

C. Capture γ-Ray Coincidence Studies

To remove ambiguities which are present in any level scheme based primarily on singles spectra, coincidences between low-energy transitions were studied with the coincidence capture γ-ray facility at Los Alamos.

The general features of this facility have been described in previous papers.[17] A neutron beam about 1 cm in diameter, with an intensity of 3×10^6 n/sec, impinged upon a 167-mg ^{187}Re target, which was placed outside the biological shield of the reactor. The two Ge(Li) detectors used in these measurements had active volumes of 35 and 45 cm^3. The detectors were placed 180° apart and on a line perpendicular to the neutron beam. A thin ceramic disk containing ^{6}LiF was placed between each detector and the target to absorb scattered thermal neutrons. In this 180° geometry, coincidences can result from the backscattering

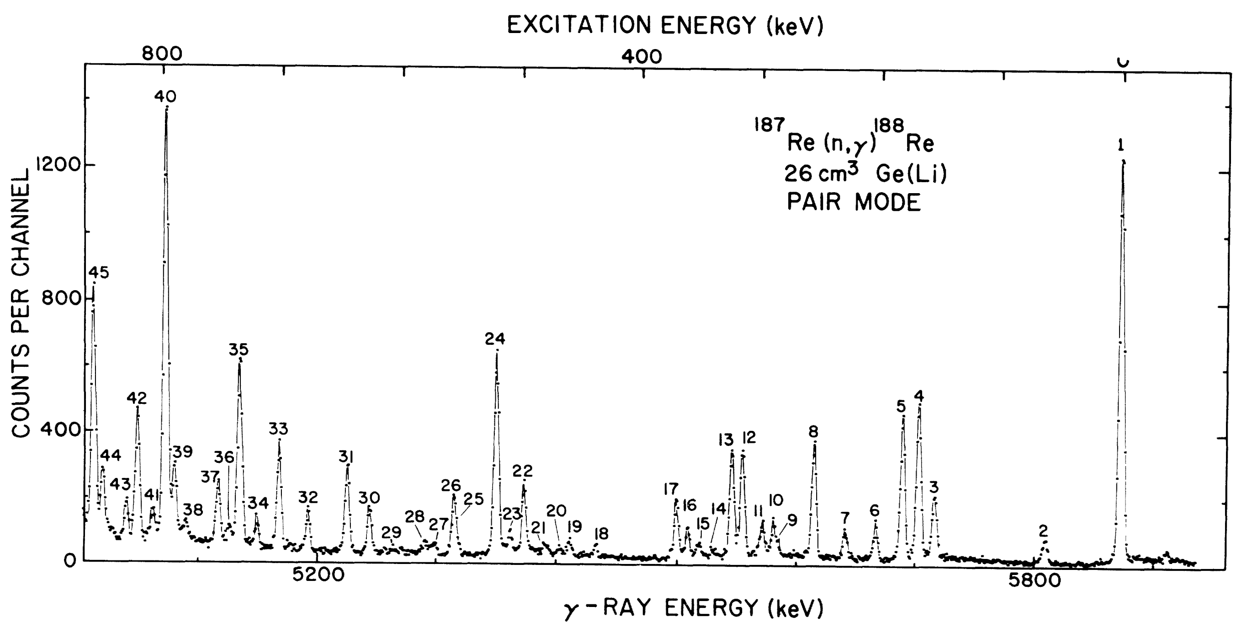

FIG. 2. High-energy γ-ray spectrum from the reaction ^{187}Re$(n,\gamma)^{188}$Re observed with the Los Alamos Ge(Li) pair spectrometer. The lines are numbered to correspond to Table I.

of a single photon from one detector to the other. An effort has been made to properly identify all such spurious coincidence peaks.

A 1600×1600-channel, two-parameter, magnetic-tape-storage analyzer was used to record the coincidence spectra. The data were sorted by scanning the magnetic tapes to obtain the spectrum in coincidence with selected transitions. Typical coincidence spectra are shown in Fig. 3, and a summary of the results is presented in Table III.

D. (*d, p*) Studies

The Florida State University tandem Van de Graaff accelerator,[18] in conjunction with a Browne-Buechner[19] broad-range magnetic spectrograph, comprises the experimental assembly by which the (d, p) reactions were studied. A monoenergetic beam of 12-MeV deuterons bombarded a target containing the separated isotope ^{187}Re. The emergent proton groups were analyzed by the spectrograph magnet, and their paths were permanently recorded by an array of four 2×10-in. 50-μ nuclear-emulsion plates. These plates were covered with aluminum foil 0.005 in. thick in order to stop elastically scattered deuterons. To prevent any possible deterioration of the emulsion from destroying or distorting the definition of the tracks, the plates were developed immediately after each exposure. The developed plates were subsequently scanned for proton tracks per $\frac{1}{2}$×8-mm strips with dark-field illuminated microscopes equipped with calibrated stages. The data presented here are given as the number of proton tracks per $\frac{1}{2}$-mm strip of plate as a function of distance along the magnet focal curve.[20]

The target used in these experiments was composed of metallic rhenium and was prepared with the Florida State University isotope separator.

TABLE I. High-energy capture γ-ray energies and intensities from the reaction ^{187}Re$(n, \gamma)^{188}$Re.

No.	γ-ray energy (keV)	Excitation energy (keV) [a]	Intensity (γ/1000 neutrons capture) [b]	No.	γ-ray energy (keV)	Excitation energy (keV) [a]	Intensity (γ/1000 neutrons capture) [b]
1	5871.59±0.3	0	7.30±1.50	28	5289.76±0.8	581.85±0.70	0.15±0.04
2	5807.81±0.4	63.78±0.20	0.40±0.08	29	5263.22±1.0	608.39±1.00	0.13±0.04
3	5715.51±0.3	156.09±0.10	1.14±0.20	30	5242.83±0.4	628.79±0.20	0.84±0.20
4	5702.10±0.3	169.50±0.10	2.65±0.50	31	5224.54±0.4	647.08±0.30	1.57±0.32
5	5688.84±0.3	182.76±0.10	2.30±0.50	32	5191.78±0.6	679.83±0.50	0.61±0.13
6	5666.30±0.4	205.30±0.20	0.47±0.10	33	5167.60±0.4	704.02±0.30	1.78±0.38
7	5640.74±0.4	230.86±0.15	0.41±0.10	34	5148.94±0.5	722.67±0.40	0.37±0.09
8	5614.72±0.3	256.88±0.10	2.00±0.40	35	5134.77±0.4	736.84±0.30	3.34±0.70
9	5584.20±0.8	287.40±0.70	0.11±0.04	36	5126.30±0.8	745.32±0.70	0.33±0.07
10	5580.92±0.4	290.68±0.20	0.63±0.15	37	5117.12±0.4	754.49±0.30	1.01±0.21
11	5571.52±0.4	300.09±0.20	0.62±0.13	38	5088.64±1.0	782.98±1.00	0.30±0.09
12	5554.78±0.4	316.82±0.20	1.96±0.40	39	5080.28±0.5	791.33±0.40	1.30±0.27
13	5545.86±0.4	325.74±0.20	1.76±0.40	40	5073.16±0.4	798.45±0.20	8.00±1.60
14	5528.43±0.9	343.17±0.80	0.10±0.10 [c]	41	5062.79±0.7	808.83±0.60	0.47±0.11
15	5518.10±1.0	353.50±1.00	0.18±0.05	42	5049.29±0.4	822.32±0.30	2.10±0.43
16	5509.03±0.4	362.57±0.20	0.41±0.10	43	5040.06±0.5	831.55±0.40	0.63±0.13
17	5499.56±0.3	372.04±0.12	1.00±0.20	44	5020.58±0.5	851.04±0.40	1.27±0.27
18	5432.21±0.6	439.40±0.50	0.14±0.05	45	5012.67±0.4	858.96±0.30	4.50±0.90
19	5409.48±0.5	462.13±0.40	0.17±0.05	46	5000.76±0.5	870.86±0.40	2.27±0.47
20	5401.22±1.0	470.38±1.00	0.07±0.03	47	4987.92±0.5	883.70±0.50	2.21±0.46
21	5389.51±0.5	482.09±0.35	0.15±0.04	48	4973.13±0.7	898.49±0.60	1.98±0.42
22	5371.91±0.3	499.70±0.10	1.20±0.24	49	4958.72±0.7	912.89±0.60	1.79±0.37
23	5359.72±0.5	511.89±0.25	0.34±0.07	50	4945.64±0.3	···	(~20) [d]
24	5348.69±0.3	522.92±0.10	3.90±0.80	51	4927.19±0.6	944.43±0.50	0.51±0.11
25	5314.78±1.0	556.83±0.90	0.29±0.18	52	4916.28±0.4	955.34±0.30	1.03±0.22
26	5313.29±1.0	558.32±0.90	0.85±0.40	53	4893.36±0.4	978.26±0.30	1.07±0.22
27	5296.49±0.5	575.12±0.40	0.19±0.05	54	4888.55±0.4	983.07±0.30	2.06±0.42

[a] Based on a neutron binding energy of 5871.59 keV and corrected for nuclear recoil.
[b] Based on σ_c = 73 b (Ref. 11).
[c] Existence of this line is questionable.
[d] ^{13}C(n, γ).

TABLE II. The low-energy neutron capture γ-ray data. The multipolarity column lists the principle multipole component according to Suarez *et al.* (Ref. 6): The assignments are discussed in Sec. III.

E (keV)	ΔE (eV)	$I_\gamma/100n$	$\Delta I_\gamma/I_\gamma$ (%)	Multipolarity	Assignment (keV)	Comments
46.692	8	0.09	20	$M1$		
53.439	12	0.024	30			
63.583	3	11	15	$M1$	63.6	
65.137	18	0.24	10			
68.037	18	0.17	10			
72.060	20	0.55	10		362.7	
74.864	3	1.75	10	$E1$	230.9	
85.322	30	0.048	20		290.7	
87.481	3	0.15	15	$M1$	256.9, 372.1	
89.866	30	0.042	25			
92.355	3	0.33	15	$E1$?	300.2	
92.464	3	1.1	10	$M1$	156.1	
93.577	3	0.29	10	$M1$		
94.21	30	0.16	15			
102.51	20	0.016	30			
102.69	20	0.029	30			
105.862	3	2.50	8	$M1$	169.4	
107.425	3	0.36	8	$M1$	470.1	
108.19	30	0.022	25			
108.64	30	0.009	35			
111.590	3	0.60	8	$M1$?	316.9	
111.681	3	0.55	8	$M1$?		
112.14	50	0.01	30			Questionable line
114.563	5	0.14	10	$M1$		
115.156	4	0.37	10	$M1$	284.6, 372.1	
115.33	30	0.031	3			
116.52	30	0.006	35			
117.13	30	0.019	20		628.9	
117.74	30	0.031	250		287.1, 470.1	
119.26	33	0.037	20			
119.82	33	0.009	35			
121.52	33	0.034	20		352.4	
123.27	33	0.017	25		680.1	Complex
123.38	33	0.017	25			Complex
125.83	33	0.006	35			Questionable line
127.729	4	0.36	8			
128.13	33	0.008	25			
128.56	33	0.14	10		284.6	
129.976	5	0.12	15		360.9	
130.76	33	0.03	30		300.2	
131.079	5	0.560	10	$M1$	287.1	
131.66	35	0.017	30			
132.822	5	0.180	15			
133.19	35	0.021	30			
135.32	40	0.026	30			
135.49	40	0.055	4			
135.70	45	0.02	30		575.4	
137.48	45	0.015	25			
138.725	5	0.25	15	$M1$	346.6	
140.965	5	0.20	15	$M1$		

TABLE II *(Continued)*

E (keV)	ΔE (eV)	$I_\gamma/100n$	$\Delta I_\gamma/I_\gamma$ (%)	Multipolarity	Assignment (keV)	Comments
141.24	40	0.08	15		346.6	
141.757	5	1.500	9	$M1$	205.3	
142.710	40	0.015	25		429.8	
143.127	5	0.12	15		325.9	
144.166	7	0.07	15		300.2	
145.155	5	0.37	10	$M1$	429.8, 462.1	
145.721	5	0.64	8	$M1$		
146.60	45	0.01	30		628.9	
146.99	45	0.01	30			
147.446	45	0.035	25		316.9	Questionable line
149.570	45	0.01	30			Questionable line
150.972	5	0.32	10		523.0	
151.120	45	0.110	20			
152.560	45	0.02	20			
153.220	45	0.007	30		499.7	Questionable line
153.670	45	0.01	30			
154.110	50	0.015	25			Complex
155.045	4	22	8	$E2$		^{188}Os
156.010	55	0.10	15		156.0	
156.421	5	0.67	8	$M1$	325.9	
157.194	5	0.41	8	$M1$		
158.30	40	0.04	15			
158.709	40	0.078	10		628.9	
159.208	5	0.20	15			Complex
161.074	8	0.10	10		448.2	
161.90	50	0.007	30			Questionable line
162.35	40	0.04	10			
163.18	40	0.027	15			
163.63	50	0.013	30		448.2	
165.24	50	0.009	35			
166.74	40	0.037	15		372.1	
167.327	4	1.950	8	$E1$	230.9	
167.910	4	0.066	15			
169.47	60	0.09	15		169.4	
169.84	60	0.031	30		325.9	
170.83	60	0.055	15			Complex
170.95	60	0.062	30			Complex
171.20	60	0.019	30			Complex
172.25	60	0.019	30			
173.006	6	0.096	10			
174.72	70	0.015	35			
175.27	70	0.006	35			
176.280	50	0.028	20			
177.143	8	0.09	15			
178.134	6	0.34	10		360.9	
178.839	6	0.13	15		541.6	
180.60	50	0.041	15			
181.58	50	0.06	15			
181.942	6	0.48	8		482.2	
183.04	50	0.028	20		352.4	
184.250	65	0.006	35			
185.638	7	0.095	10			
186.71	50	0.02	30			
187.83	50	0.073	15			
188.813	7	1.3	8	$E1$	360.9	

TABLE II *(Continued)*

E (keV)	ΔE (eV)	$I_\gamma/100n$	$\Delta I_\gamma/I_\gamma$ (%)	Multipolarity	Assignment (keV)	Comments
189.320	45	0.026	30		372.1, 550.2	
190.004	9	0.14	15			
190.374	7	0.22	15	$M1$		
190.83	50	0.022	25			
191.58	50	0.019	30			Complex
191.74	50	0.019	30			Complex
192.55	50	0.006	35			Questionable line
193.346	10	0.60	10	$M1$	256.9	
196.36	55	0.105	15		352.4	
197.17	55	0.018	30		523.0	
197.55	55	0.023	30			
199.512	5	1.35	8	$M1$	499.7	
201.56	60	0.011	25			
202.00	60	0.007	30			
202.63	60	0.05	20		372.1	
205.349	8	0.57	10		205.3	
206.05	90	0.014	30		523.0	
206.676	13	0.073	15		362.7	
207.849	5	6.000	8	$E1$	207.9	
208.844	8	1.3	8	$M1$	439.8	
211.52	8	0.36	15		511.7	
213.28	90	0.011	25		470.1	
214.10	90	0.018	30			
216.017	7	0.36	15		372.1	
217.098	7	0.27	15			
218.29	60	0.026	30			
218.80	60	0.023	30			
219.449	8	0.86	2	$M1$	582.2	
221.35	60	0.031	25			
222.96	70	0.031	25		575.4	
223.60	70	0.11	10		287.1	
224.60	70	0.024	25		541.6	
225.13	70	0.02	30			
225.94	70	0.007	30			Questionable line
227.082	7	3.0	8	$M1$	290.7	
228.62	70	0.055	20			
229.62	70	0.016	30			
230.82	70	0.016	30			
231.92	70	0.041	25			Complex
232.35	70	0.13	15			
233.28	70	0.027	20			
234.39	70	0.037	20		439.8	
235.86	70	0.099	15			
236.647	8	2.3	8	$E1$, $E2$	300.2	
238.369	15	0.195	15		523.0	
240.26	110	0.055	20			Complex
240.43	70	0.032	30			Complex
241.30	70	0.055	20		541.6	
241.93	70	0.041	30			
245.13	70	0.041	30			
246.28	80	0.08	20		609.0	

TABLE II *(Continued)*

E (keV)	ΔE (eV)	$I_\gamma/100n$	$\Delta I_\gamma/I_\gamma$ (%)	Multipolarity	Assignment (keV)	Comments
247.15	80	0.08	20		429.7	
248.72	80	0.012	35			
251.239	8	1.47	10	$M1$	482.2	
252.974	17	0.10	30			
256.924	10	1.3	10	$M1$	256.9	
258.57	90	0.017	30		575.4	
260.15	90	0.013	30			
262.761	13	0.12	15			
263.67	140	0.03	30			
264.75	140	0.022	30		470.1	
266.175	20	0.11	15		628.9	
266.85	100	0.082	20			
268.95	140	0.008	25			
271.07	100	0.042	30			
272.35	150	0.009	35			
273.59	100	0.082	30			
274.317	11	1.3	10	$M1$	482.2	
275.510	9	0.9	10	$M1$	757.7	
276.82	100	0.08	15		482.2	
277.96	100	0.08	15			
278.40	100	0.014	30			Complex
280.28	100	0.01	30			Complex
280.76	100	0.01	30			Complex
281.10	100	0.01	30			Questionable line
282.23	120	0.024	30		628.9	Complex
282.98	120	0.01	30			Questionable line
283.67	120	0.01	30		439.8	Questionable line
284.585	16	0.36	15		647.3	
285.54	120	0.029	30			Complex
286.70	120	0.029	30			
287.86	120	0.13	15			Complex
290.669	13	6.4	5	$M1$	290.7	
291.488	10	1.25	5		582.2	
293.82	120	0.096	15			
297.834	180	0.026	30			
299.125	30	0.20	7	$M1$	362.7	
300.210	11	1.3	5		300.2	
306.11	190	0.034	30		462.1	
308.440	180	0.096	15		372.1	Complex
310.07	190	0.02	30			Questionable line
310.86	190	0.014	30		541.6	Questionable line
312.73	280	0.175	8			
317.35	140	0.11	20		680.1	
318.366	40	0.23	8		609.0	
320.94	140	0.20	15			Complex
322.79	210	0.038	30			
323.94	210	0.038	30			
325.50	140	0.13	15			
328.38	220	0.064	20		628.9	
330.35	220	0.064	20			

TABLE II *(Continued)*

E (keV)	ΔE (eV)	$I_\gamma/100n$	$\Delta I_\gamma/I_\gamma$ (%)	Multipolarity	Assignment (keV)	Comments
333.55	220	0.055	20			Questionable line
335.58	140	0.14	20			
337.368	44	0.14	25			
338.223	44	0.49	15			
340.26	230	0.04	30		523.0	
341.653	22	0.17	15			
343.67	230	0.03	30			
344.74	230	0.06	30			
346.15	250	0.04	30			Complex
346.69	250	0.06	30			Complex
348.79	250	0.06	30		556.8	Complex
352.127	40	0.25	15		609.0	
354.36	250	0.17	15			
358.777	35	0.30	15			
360.40	200	0.19	15			
362.66	200	0.94	10	$M1$	362.7	
363.04	200	0.18	30			Complex
368.99	270	0.046	30			
370.61	270	0.078	30			
372.15	200	0.14	25		372.1	
374.30	200	0.11	30		582.2	
375.522	30	0.66	10			
376.80	200	0.11	15		582.2	
379.15	200	0.07	40			Complex
381.78	200	0.05	40			Complex
386.21	50	0.29	15			
389.46	60	0.22	15		680.1	
394.08	300	0.066	30			Complex
396.62	300	0.034	30			Questionable line
399.99	200	0.055	30			Complex
401.21	300	0.08	30			
403.85	200	0.07	30			
406.506	65	0.37	20		470.1	
410.61	220	0.07	30			
413.88	220	0.15	25			
420.19	220	0.10	30			
423.56	220	0.16	25		628.9	Complex
425.95	220	0.21	25		582.2	Complex
426.72	220	0.13	30			Complex
428.77	220	0.16	25			
431.62	220	0.25	30			Complex
432.29	220	0.14	30			Complex
434.23	220	0.10	30			Complex
437.72	260	0.29	25			
439.660	260	0.13	30			Complex
440.960	380	0.11	30			Complex
441.070	260	0.29	25			
444.20	270	0.14	30			
449.80	270	0.33	25			Complex
454.15	280	0.17	30			Complex

TABLE II *(Continued)*

E (keV)	ΔE (eV)	$I_\gamma/100n$	$\Delta I_\gamma/I_\gamma$ (%)	Multipolarity	Assignment (keV)	Comments
455.46	400	0.17	30			Complex
456.46	280	0.17	30			Complex
460.05	280	0.11	30			Complex
463.64	420	0.07	30			
466.38	450	0.11	30			
469.26	280	0.12	30			
473.14	450	0.06	30			Questionable line
474.75	280	0.27	20			
478.033	35	0.90	30			^{188}Os
479.90	300	0.05	40			Complex
482.11	450	0.03	40			Questionable line
486.09	300	0.05	40			Complex
487.21	450	0.03	40			Complex
491.32	450	0.10	300			
493.05	300	0.18	30		556.8	
496.41	500	0.033	40			Questionable line
499.30	380	0.20	30			
500.74	380	0.14	30			
504.34	550	0.05	30			
507.55	380	0.13	30			
518.64	380	0.25	30		582.2	
522.47	580	0.11	30			Questionable line
524.05	580	0.11	30			Questionable line
525.69	580	0.07	30			Questionable line
529.21	580	0.05	30			Complex
537.39	400	0.11	30			Complex
542.97	400	0.12	30			
548.86	400	0.16	30			
554.43	400	0.27	25			
557.35	400	0.17	30		556.8	
560.75	400	0.08	30			Questionable line
565.80	650	0.24	30			
577.96	700	0.12	30			
580.50	700	0.37	30			Complex
586.70	700	0.15	30			
596.03	700	0.19	30			
599.93	740	0.19	30			Complex
602.57	740	0.40	30			Complex
609.23	500	0.72	30		609.0	
615.69	750	0.20	30			Complex
626.55	500	0.64	25			
633.036	100	1.5	25			^{188}Os
646.64	600	0.22	30			
662.900	600	0.46	30			
665.960	900	0.23	30			Complex
673.00	900	0.23	30			
676.21	900	0.15	30			Questionable line
684.20	900	0.31	30			
694.12	950	0.25	30			Complex
701.42	1000	0.42	30			
709.55	1000	0.21	30			
714.78	700	0.43	30			Complex
725.68	1100	0.17	30			Complex
744.20	800	0.34	30			Complex
794.90	800	0.53	30			
829.23	1300	0.64	30			Complex

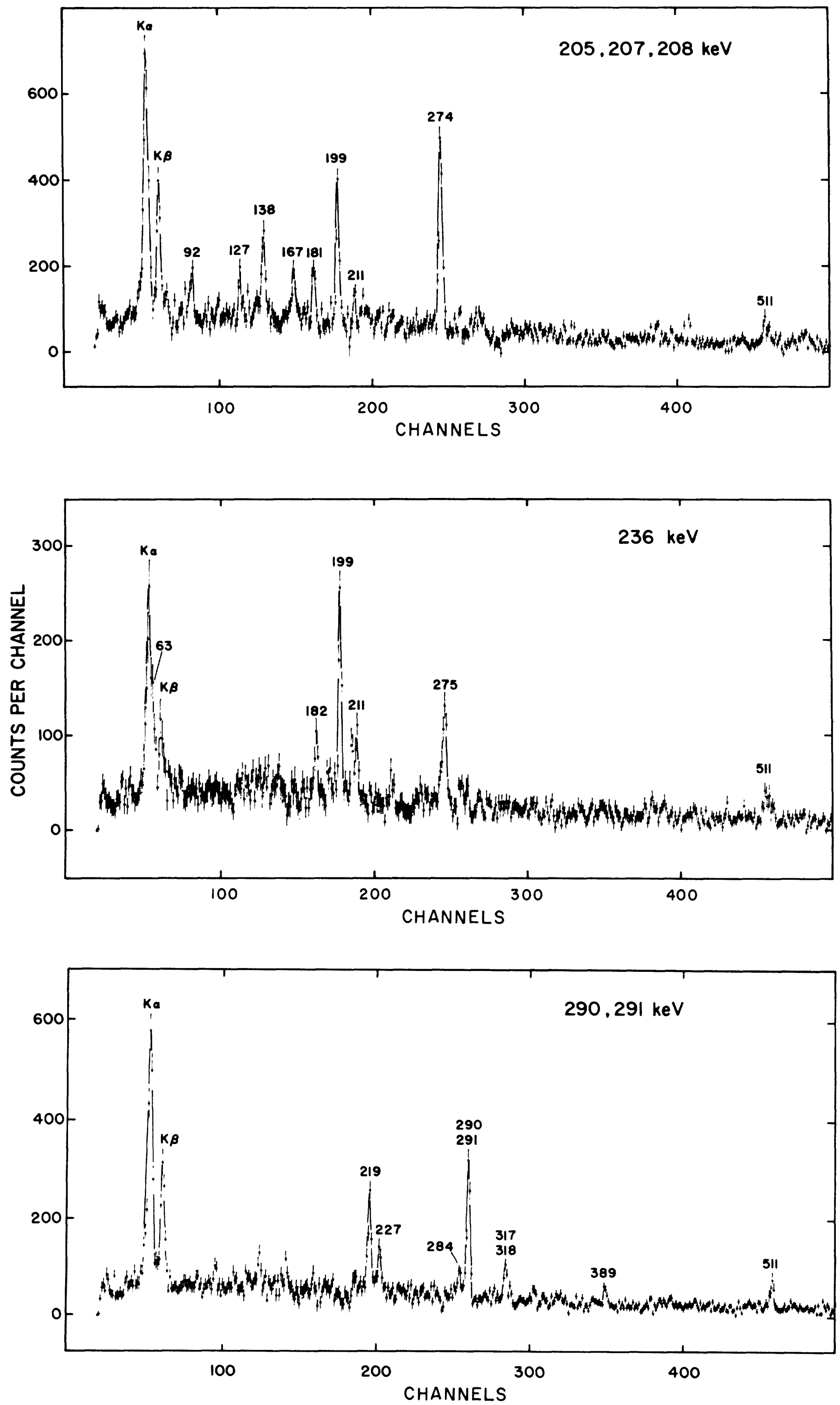

FIG. 3. Representative capture γ-ray coincidence spectra showing the low-energy γ-ray spectrum in coincidence with lines at about 207, 236, and 290 keV, respectively. A spectral background has been subtracted from the illustrated data.

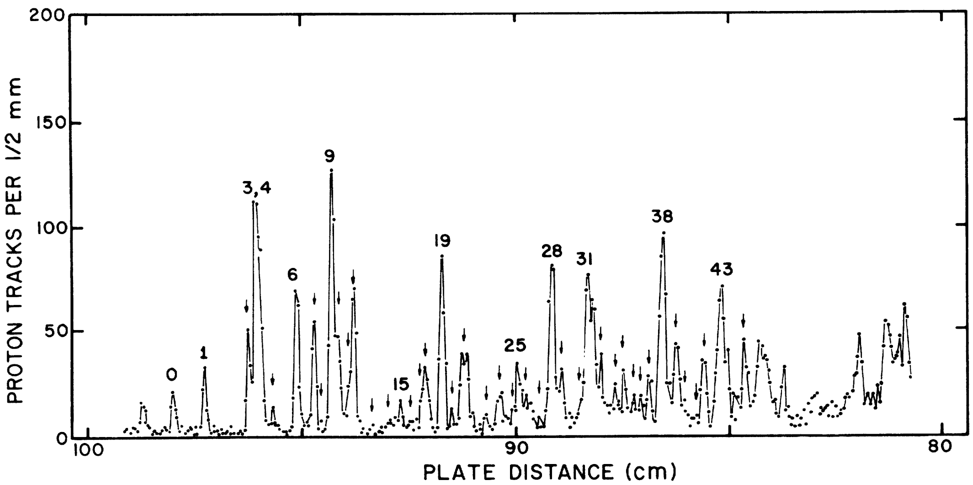

FIG. 4. Proton spectrum from the reaction $^{187}Re(d, p)^{188}Re$ observed at 55°.

TABLE III. $^{187}Re(n, \gamma\gamma)^{188}Re$ coincidence measurements. Observed coincidence between two γ rays is indicated by an x at the appropriate intersection. A bar beneath an x indicates that the observed coincidence is understood in terms of the level schemes of Figs. 7–9.

γ-ray energy (keV)	105.9	156.4	167.3	188.8	199.5	205.3 207.8 208.8	227.1	236.6	251.2	256.9	274.3 275.5	290.7 291.5	300.2
63.5	$\underline{x}$		$\underline{x}$				$\underline{x}$	$\underline{x}$					
92.4						$\underline{x}$							
105.9		$\underline{x}$											
111.6						$\underline{x}$							
115.2										$\underline{x}$			
127.7						x					x		
138.7						$\underline{x}$							
156.4	$\underline{x}$												
167.3						$\underline{x}$			$\underline{x}$				
178.1	$\underline{x}$												
181.9						$\underline{x}$		$\underline{x}$					$\underline{x}$
189.3				$\underline{x}$									
199.5						$\underline{x}$		$\underline{x}$					$\underline{x}$
207.8 [a]					$\underline{x}$						$\underline{x}$		
208.8 [a]			$\underline{x}$										
211.5						$\underline{x}$		$\underline{x}$					$\underline{x}$
219.4							$\underline{x}$					$\underline{x}$	
227.1												$\underline{x}$	
236.6					$\underline{x}$						$\underline{x}$		
251.2			$\underline{x}$								$\underline{x}$		
274.3 [a]						$\underline{x}$					$\underline{x}$		
275.5 [a]								$\underline{x}$	$\underline{x}$		$\underline{x}$		$\underline{x}$
284.6							$\underline{x}$					$\underline{x}$	
290.7 [a]												$\underline{x}$	
291.5 [a]							$\underline{x}$					$\underline{x}$	
300.2					$\underline{x}$						$\underline{x}$		
317.4 [a]							$\underline{x}$					$\underline{x}$	
318.4 [a]							$\underline{x}$					$\underline{x}$	
389.5												$\underline{x}$	

[a] This line is not completely resolved from a nearby line of similar intensity. The coincidence as shown is that most consistent with all available data.

TABLE IV. Excitation energies and cross sections from the reaction ^{187}Re$(d,p)^{188}$Re. For a detailed discussion of the data listed below "Interpretation" see Sec. III.

Experimental data					Interpretation					
Level No.	(d,p) energy [a] (keV)	Error (keV)	^{187}Re(d,p) σ (μb) [b] 55°	116°	Assigned level energy (keV)	$I^{\pi}K$	Nilsson configuration π	ν	Theoretical σ (μb) 55°	116°
0	0.0	2	25	11	0.0	$1^{-}1$	$\frac{5}{2}^{+}[402\uparrow]$	$\frac{3}{2}^{-}[512\downarrow]$	41	12
1	61.5	2	32	16	63.58	$2^{-}1$	$\frac{5}{2}^{+}[402\uparrow]$	$\frac{3}{2}^{-}[512\downarrow]$	38	13
2	154.3	3	40	32	156.05	$3^{-}1$	$\frac{5}{2}^{+}[402\uparrow]$	$\frac{3}{2}^{-}[512\downarrow]$	23	9.5
3	169.8 [c]	4	≥117 [d]	≤75 [d]	169.44	$3^{-}3$	$\frac{5}{2}^{+}[402\uparrow]$	$\frac{1}{2}^{-}[510\uparrow]$	42	13
					172.07	$6^{-}6$	$\frac{5}{2}^{+}[402\uparrow]$	$\frac{7}{2}^{-}[503\uparrow]$	106	55
4	181.8 [c]	4	≤81 [d]	≥12 [d]	182.76	$4^{-}4$	$\frac{5}{2}^{+}[402\uparrow]$	$\frac{3}{2}^{-}[512\downarrow]$	90	29
5	205.1	3	11	8	205.34	$2^{-}2$	$\frac{5}{2}^{+}[402\uparrow]$	$\frac{9}{2}^{-}[505\downarrow]$	4.7	4.1
6	255.1	2	74	24	256.92	$2^{-}2$	$\frac{5}{2}^{+}[402\uparrow]$	$\frac{1}{2}^{-}[510\uparrow]$	32	9.5
					284.60	$4^{-}3$	$\frac{5}{2}^{+}[402\uparrow]$	$\frac{1}{2}^{-}[510\uparrow]$	30	10
					287.13	$4^{-}1$	$\frac{5}{2}^{+}[402\uparrow]$	$\frac{3}{2}^{-}[512\downarrow]$	9	4.5
7	285.8	2	51	30	290.67	$1^{-}1$	$\frac{5}{2}^{+}[402\uparrow]$	$\frac{7}{2}^{-}[503\uparrow]$	40	20
8	(306) [e]	8	<3	<6	316.93	$3^{-}2$	$\frac{5}{2}^{+}[402\uparrow]$	$\frac{9}{2}^{-}[505\downarrow]$	3.1	2.6
9	321.2 [c]	3	~128 [d]	~56 [d]	325.86	$4^{-}4$	$\frac{5}{2}^{+}[402\uparrow]$	$\frac{3}{2}^{-}[501\uparrow]$	315	93
10	335.7 [c]	4	~45 [d]	~38 [d]	~336	$5^{-}4$	$\frac{5}{2}^{+}[402\uparrow]$	$\frac{3}{2}^{-}[512\downarrow]$	20	10
11	357	5	22	46	362.72	$2^{-}1$	$\frac{5}{2}^{+}[402\uparrow]$	$\frac{7}{2}^{-}[503\uparrow]$	37	19
12	368	3	77		372.08	$3^{-}1$	$\frac{5}{2}^{+}[402\uparrow]$	$\frac{1}{2}^{-}[510\uparrow]$	31	10
13	(408)	8	<4	<6	...	...	...	...	...	...
					429.77	$5^{-}3$	$\frac{5}{2}^{+}[402\uparrow]$	$\frac{1}{2}^{-}[510\uparrow]$	4.2	2.5
14	443	5	<6	<3	439.75	$3^{+}3$	$\frac{5}{2}^{+}[402\uparrow]$	$\frac{11}{2}^{+}[615\uparrow]$	0	0
					448.21	$5^{-}1$	$\frac{5}{2}^{+}[402\uparrow]$	$\frac{3}{2}^{-}[512\downarrow]$	2.5	1.5
15	465	3	~12	<12	462.08	$4^{-}2$	$\frac{5}{2}^{+}[402\uparrow]$	$\frac{9}{2}^{-}[505\downarrow]$	1.6	1.2
					470.14	$3^{-}1$	$\frac{5}{2}^{+}[402\uparrow]$	$\frac{7}{2}^{-}[503\uparrow]$	21	11
16	489	5	<5	<10	499.72	$3^{+}0$	$\frac{9}{2}^{-}[514\uparrow]$	$\frac{9}{2}^{-}[505\downarrow]$	0	0
17	(512) [c]	6	≤19 [d]	30	511.73	$4^{+}0$	$\frac{9}{2}^{-}[514\uparrow]$	$\frac{9}{2}^{-}[505\downarrow]$	0	0
18	521 [c]	4	≥28 [d]		523.00	$4^{-}2$	$\frac{5}{2}^{+}[402\uparrow]$	$\frac{1}{2}^{-}[510\uparrow]$	12	4.5
19	555	3	85	48	556.83	$1^{-}1$	$\frac{5}{2}^{+}[402\uparrow]$	$\frac{3}{2}^{-}[501\uparrow]$ [f]	154	45
20	588 [c]	...	33	10	582.17	$1^{-}1$				
					575.45	$4^{+}3$	$\frac{5}{2}^{+}[402\uparrow]$	$\frac{11}{2}^{+}[615\uparrow]$	1.6	3.9
21	606	4	32	16	609.04	$2^{-}1$	$\frac{5}{2}^{+}[402\uparrow]$	$\frac{3}{2}^{-}[501\uparrow]$ [f]	118	38
22	(647)	8	7	6	647.30	$2^{-}1$				
23	674	4	20	9	680.11	$3^{-}1$	$\frac{5}{2}^{+}[402\uparrow]$	$\frac{3}{2}^{-}[501\uparrow]$ [f]	50	17
24	(703)	8	9	11						
25	717	3	21	21						
26	733 [c]	4	30	22						
27	761	4	6	10						
28	788	2	101	47						

TABLE IV (*Continued*)

Experimental data					Interpretation						
Level No.	(d,p) energy [a] (keV)	Error (keV)	^{187}Re(d,p) σ (μb) [b] 55°	116°	Assigned level energy (keV)	$I^{\pi}K$	Nilsson configuration π	ν	Theoretical σ (μb) 55°	116°
29	813	6	30	14						
30	844	5	14	9						
31	866	2	78	37						
32	895	6	28	11						
33	926	3	22	19						
34	946	3	25	19						
35	965	4	16	5						
36	981	6	14	11						
37	996	3	28	18						
38	1029	3	127	87						
39	1058	3	55	28						
40	1075	5	13	12						
41	1094	5	7	10						
42	1118	5	41	31						
43	1160 [c]	7	125	59						

[a] Energy values obtained by averaging the 55 and 116° exposures.
[b] Cross sections are calculated assuming a target thickness of 60 μg/cm^2. Errors in *relative* cross sections are 20% for strong peaks; 30–50% for weak peaks.
[c] Complex line.
[d] An attempt has been made to resolve the complex line.
[e] The existence of lines shown in parentheses is questionable.
[f] These states involve both intrinsic and $|K-2|$ γ-vibrational components.

Details of the target preparation have been published elsewhere.[21] A thin film of carbon (200–300 μg/cm^2) was employed as the target substrate. This target possessed a ^{187}Re enrichment of ≈99%, and was estimated to have a thickness of 60 μg/cm^2.

The raw spectrograph data were analyzed using the computer code STRILDE[22] written for the Florida State University CDC 6400 computer. This program decomposes the observed spectra into a sum of symmetrical Gaussian distributions, each having a characteristic centroid and area, and determines the Q values and cross sections corresponding to these parameters.

The (d,p) exposures leading to ^{188}Re, averaging between 8000 and 12 000 μC, were analyzed at two angles: 55 and 116°. The 55° exposure exhibited the best energy resolution and this spectrum is shown in Fig. 4. These experiments have determined the ground-state (d,p) Q value to be 3655 ± 20 keV. The excitation energies and relative cross sections for the levels observed in the (d,p) studies are listed in Table IV. To avoid repetition of the experimental data in a later section of the paper, a theoretical interpretation of the (d,p) results, which is discussed in detail in Sec. III, is tabulated in Table III.

E. Lifetime Measurements

The existence of low-lying delayed states in ^{188}Re has been established by the delayed-coincidence measurements of Berestovoi, Kondurov, and Loginov (BKL).[4] These authors report two groups of delayed γ rays with lifetimes of 7.7 ± 0.6 nsec (62 ± 3-, 103 ± 6-, 167 ± 4-keV γ rays) and 4.4 ± 0.3 nsec (62 ± 3- and 205 ± 6-keV γ rays). Since a unique identification of these reported energies with the data of Table II did not seem to be possible, it appeared to be worthwhile to repeat the lifetime measurements and make use of the superior energy resolution available with Ge(Li) detectors.

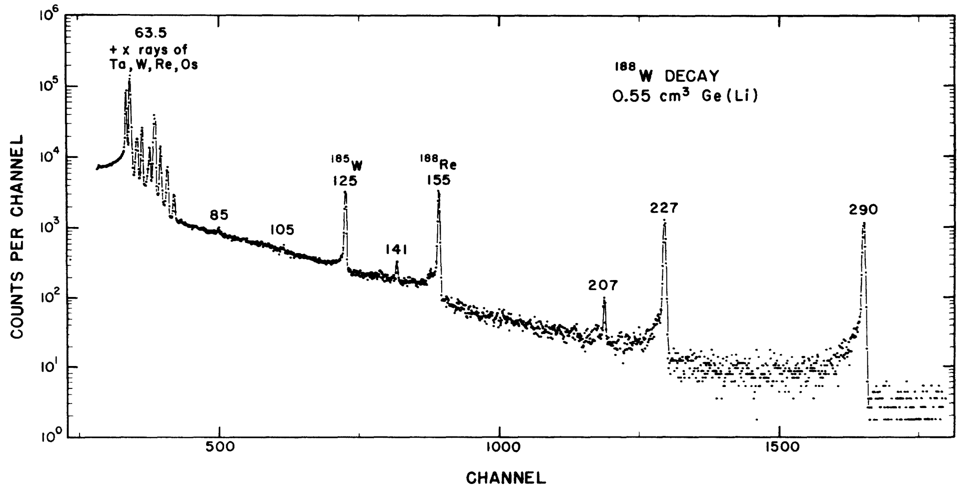

FIG. 5. γ-ray spectrum of ^{188}W observed using a 0.55-cm^3 Ge(Li) detector. The data illustrated represent the sum of several runs each of ~10-min duration which began immediately following chemical removal of the ^{188}Re daughter activity.

An arrangement of the ^{187}Re target, detectors, and neutron beam similar to that described in Sec. II C was used for the lifetime measurements. The signal from a plastic scintillator which viewed the high-energy γ-ray spectrum was used to supply a "start" pulse to a time-to-amplitude converter (TAC). The "stop" pulse was derived from a 12-cm^3 planar Ge(Li) diode by means of a commercial "extrapolated-zero strobe" circuit. Two-parameter data, each element of which consisted of a TAC output pulse and the linear signal from the Ge(Li) detector, were recorded on magnetic tape. The raw data were later sorted and analyzed with the aid of a computer. The TAC was calibrated using delay cables of known electrical length, and the calibration of the system was also verified by a measurement of the lifetime of the well-known 10-nsec isomeric state of ^{181}Ta.

The apparent half-lives of γ-ray transitions which were observably delayed are listed in Table V. The isomeric level presumed to cause the delayed transition is also listed in each case. It was not always possible to observe all of the transitions which depopulate a given level because of interference from transitions depopulating other delayed levels. For example, the 205.35-keV γ ray which depopulates the 205.3-keV level could not be separated from the more intense 207.85-keV transition, which has a nearly identical decay time.

F. β Decay of ^{188}W

An isotopically separated sample of ^{186}W was irradiated in a flux of 9×10^{13} n/cm^2/sec in the Omega West Reactor for a period of about three weeks. Two successive neutron captures in ^{186}W produced a significant amount of 60-day ^{188}W. Following irradiation, the sample was allowed to decay for approximately two weeks to eliminate the 23.9-h ^{187}W and other possible short-lived contaminant activities. Chemical purification of the sample was performed to remove contamination of 60-day

TABLE V. Delayed transitions observed in the ^{187}Re(n, γ)^{188}Re reaction.

Transition energy (keV)	Observed half-life (nsec)	Energy of isomeric level (keV)
105.86	17.6 ± 3.0	182.74
141.76	3.2 ± 0.6	205.34
167.33	20.9 ± 2.0	230.91
178.13	6.0 ± 2.5	360.88
188.81	5.2 ± 1.0	360.88
207.85	3.2 ± 0.4	207.85

TABLE VI. γ rays from the decay of ^{188}W.

Energy (keV)	Intensity (normalized)
63.58 ± 0.03	0.27 ± 0.040
85.31 ± 0.06	0.006 ± 0.002
105.85 ± 0.07	≤0.003
141.78 ± 0.03	0.016 ± 0.002
207.86 ± 0.04	0.020 ± 0.004
227.09 ± 0.02	0.55 ± 0.020
290.669 [a]	1.0 ± 0.030

[a] Energy calibration was derived from this line and the 155.045-keV line of ^{188}Os (see Table II).

^{124}Sb and 115-day ^{182}Ta. The ^{124}Sb was removed with the aid of Sb carrier, using the H_2S precipitation procedure described by Hildegrand and Lundell.[23] The ^{182}Ta removal was accomplished by the addition of Ta carrier and precipitation of Ta and W in acid solution, followed by dissolution of W in NH_4OH. Following these purification procedures, no radioactive contamination was detectable in the source except for the unavoidable 18-h ^{188}Re daughter of ^{188}W. The ^{188}Re activity was chemically separated from the desired W activity immediately before counting the sample and at 10-min intervals during the counting, using the procedure described in Ref. 1. Frequent separation is required since within the first few minutes of growth following a chemical separation the intensity of the 155-keV line, which characterizes ^{188}Re, exceeds the intensity of the strongest ^{188}W lines. To optimize the counting sensitivity for various energy regions, two separate Ge(Li) detectors were used to observe the γ-ray spectrum. A 45-cm^3 detector, which provides superior efficiency at energies of a few hundred keV and above, was used to study the higher-energy ^{188}W transitions and to search the γ-ray spectrum up to ≈ 2 MeV for impurity activities. For energies below 300 keV, the spectrum was also studied with a very small volume, high-resolution detector which has a minimal sensitivity for the intense lines with energies above 400 keV due to the ^{188}Re decay. A spectrum from this detector is shown in Fig. 5. The region of the spectrum between 56 and 71 keV is very complex, since in addition to lines from possible nuclear γ rays it contains the x-ray lines of Ta (from the decay of ^{181}W), W (from fluorescense), Re (from internal conversion), and Os (from ^{188}Re decay).

The 63.58-keV γ ray which depopulates the first excited state of ^{188}Re also occurs in this energy region. An accurate determination of the intensity of this γ transition is important because it can be used to infer the strength of the β branch which feeds the 63.5-keV level. In the earlier experiments of Burson *et al.*,[1] it was not possible to separately resolve the γ ray from the much more intense group of x-ray lines, and a complex subtraction procedure was required to estimate the intensity of the 63.5-keV transition. More direct methods could be used in analyzing the present data since the resolution (full width at half maximum = 530 eV at 60 keV) was sufficient to separate the γ ray from all lines but the weak Os $K\alpha_1$ x ray at 63.0 keV. The intensity of the 63.5-keV transition has been corrected for the intensity of the incompletely resolved x ray by appropriate scaling of the observed Os $K\beta_2'$ intensity. The energies and relative intensities of all observed transitions which are attributable to the ^{188}W decay are listed in Table VI. At least three transitions which had not been reported in previous β-decay studies are observed; the energies of these transitions are 85.31, 141.78, and 207.86 keV. In addition, a weak line at 105.8 keV is suggested by the data. A partial ^{188}Re level scheme, showing the states populated by the ^{188}W decay, is shown in Fig. 6. β-decay branching ratios and $\log ft$ values deduced from the present measurements are also presented in Fig. 6. These values were derived by normalizing the present results to the value listed in Ref. 1 for the β branch to the 290.7-keV state.

III. DISCUSSION

If the present effort is to have significance in terms of a better understanding of nuclear structure, then it is essential to distinguish clearly between what is established unambiguously by experiment and what is merely consistent with a preconceived model. Therefore, this discussion will be divided into two subsections, each with its individual level scheme. Sec. III A presents those conclusions that can be deduced from purely experimental considerations. Figure 7 summarizes this level of analysis. In Sec. III B, a detailed theoretical model is introduced, which provides an interpretation of the results of the preceding section. As is often the case, the model is used to make predictions suggesting reexamination of the experimental data, with a resulting extension of the decay scheme. A summary of the ^{188}Re level structure, as thus interpreted and extended via the Nilsson model, is shown in Figs. 8 and 9.

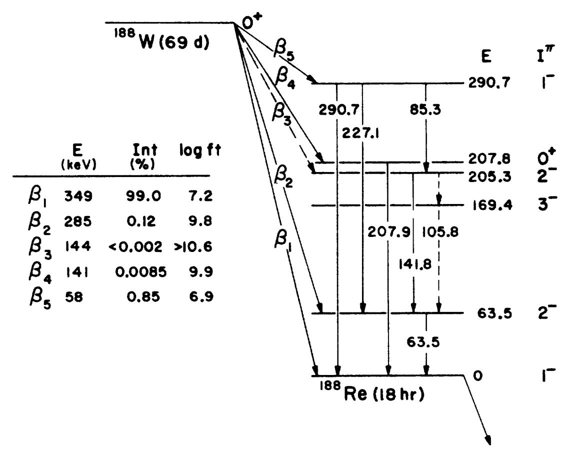

FIG. 6. Level scheme of ^{188}Re showing the levels involved in the decay of ^{188}W.

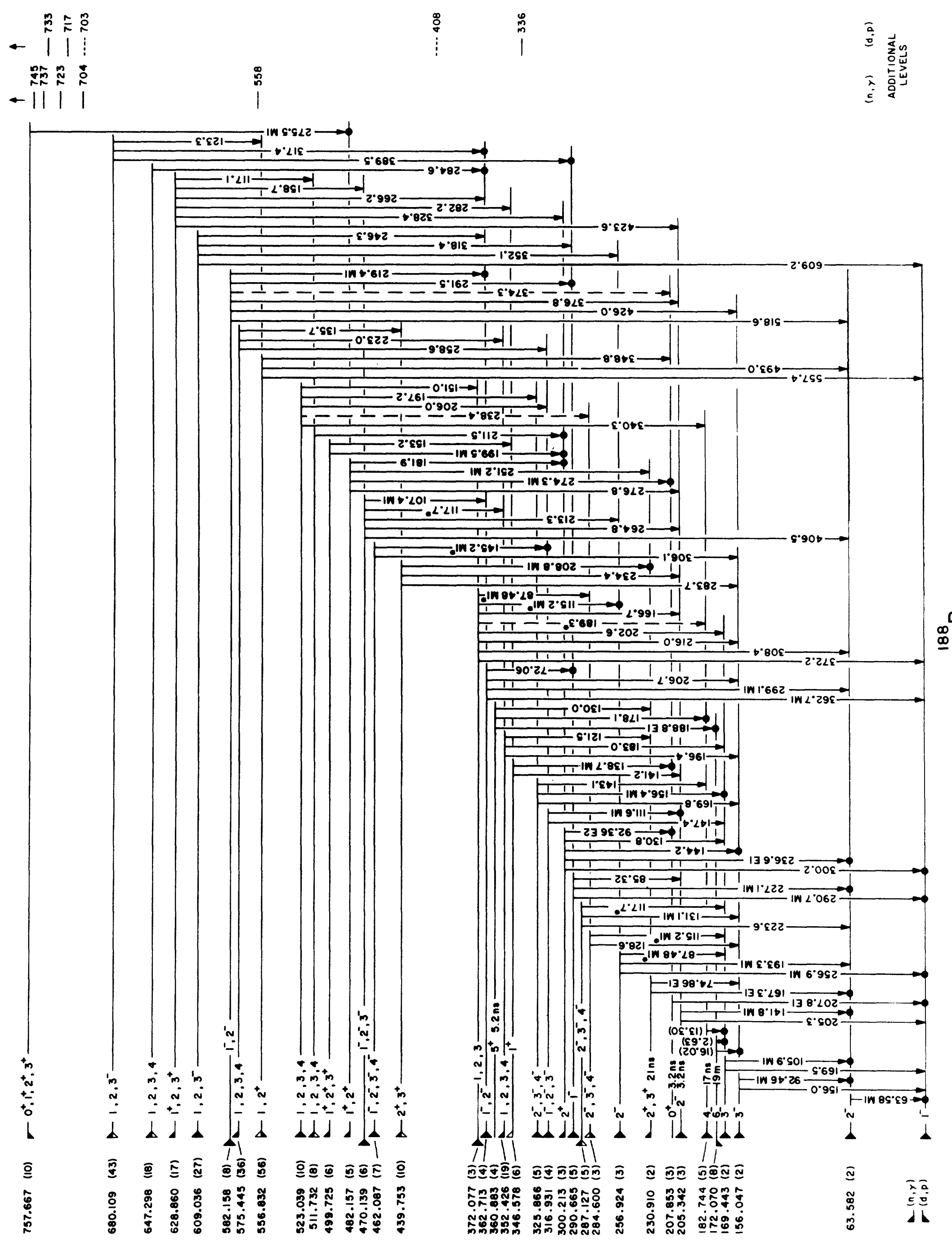

FIG. 7. Model-independent level scheme of ^{188}Re. A solid circle beneath a transition indicates that the placement is defined by the coincidence data. The indicated level energies (in keV, with associated errors in parenthesis) are those that result from a least-squares fit of the known γ-ray transition energies. A dashed level (transition) indicates that its existence (placement) is questionable. Multiply assigned transitions are denoted by an asterisk. Transition energies have been rounded to four-digit accuracy; more precise values are listed in Table II.

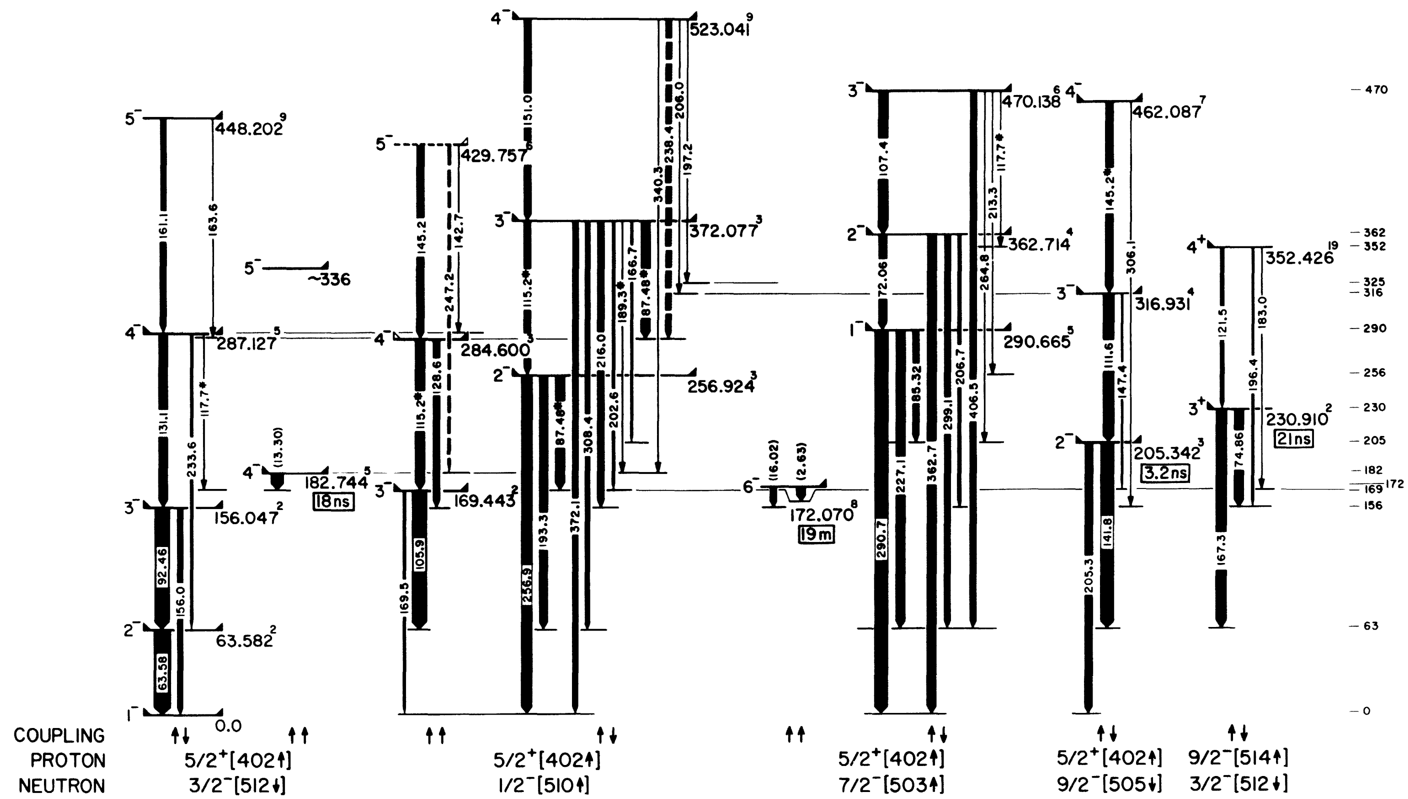

FIG. 8. Nilsson-model interpretation of ^{188}Re. The figure has been broken into two sections to improve readability. Levels which are referred to in *both* sections are summarized at the border where the two sections join. Most conventions are identical to Fig. 7. In addition, the widths of the transitions are drawn to be proportional (logarithmically) to the transition intensity (including internal conversion). The proton-neutron configuration given beneath each band is that wave-function component which is believed to predominate. High-energy (n,γ) and (d,p) reaction population of a state are indicated by flags at the left and right ends of the level, respectively.

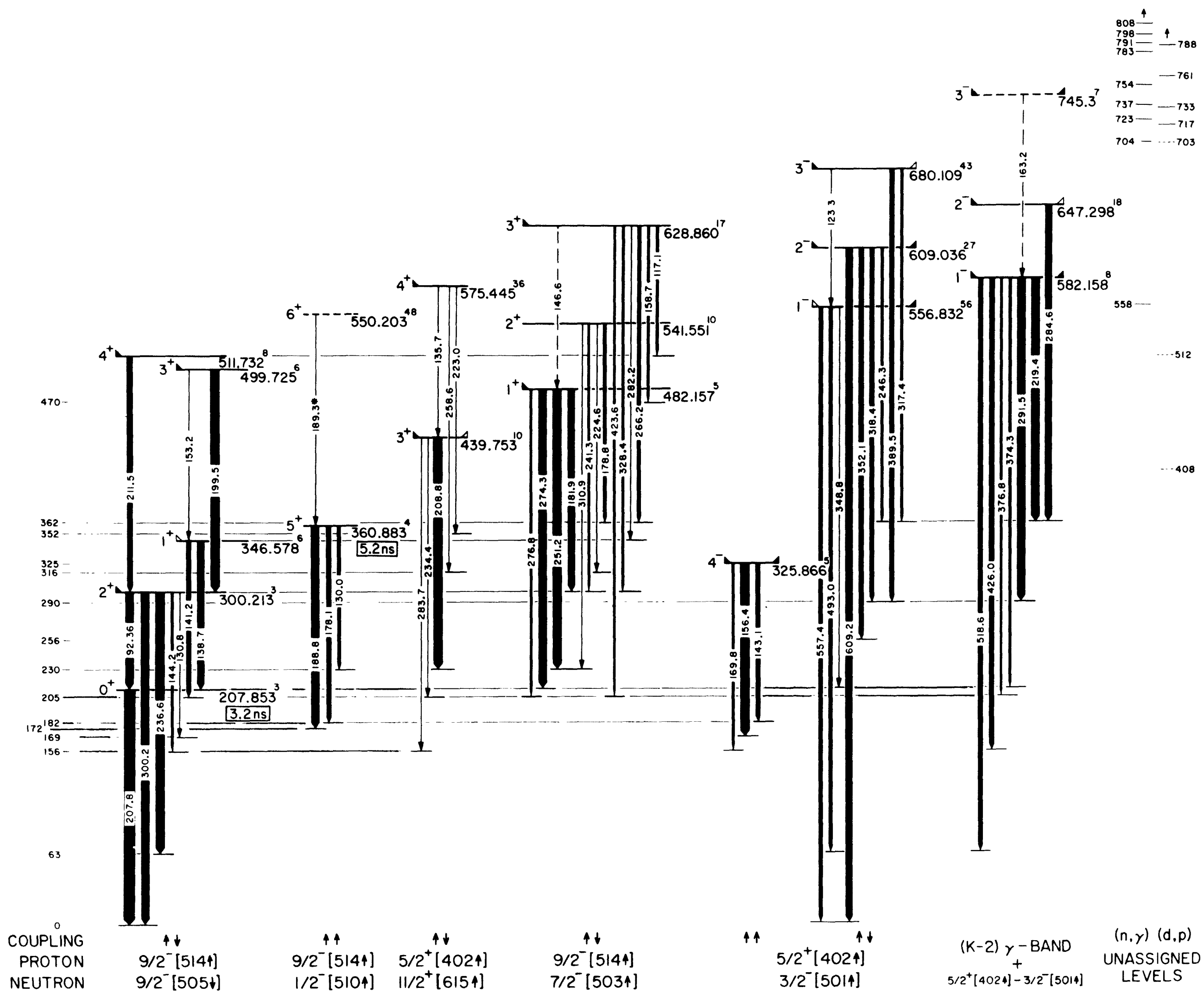

FIG. 9. Nilsson-model interpretation of ^{188}Re. The figure has been broken into two sections to improve readability. Levels which are referred to in *both* sections are summarized at the border where the two sections join. Most conventions are identical to Fig. 7. In addition, the widths of the transitions are drawn to be proportional (logarithmically) to the transition intensity (including internal conversion). The proton-neutron configuration given beneath each band is that wave-function component which is believed to predominate. High-energy (n, γ) and (d, p) reaction population of a state are indicated by flags at the left and right ends of the level, respectively.

A. Level Scheme

Data from the (d, p) and high-energy (n, γ) studies form a convenient starting point for developing a level scheme since these data serve to directly locate excited nuclear states. The very precise transition-energy information from the low-energy (n, γ) work can then be used to define more accurately the energies of the levels and to specify their depopulation modes. Use will also be made of other published information as it seems appropriate; in particular we will refer repeatedly to the multipolarity data of Suarez *et al.*[6]

1. Levels at 0.0, 63.6, and 156.0 keV

The ground state and two lowest excited states, at 63.6 and 156.0 keV, have been well established by previous studies. The spin of the ground state has been determined as 1 by the atomic-beam measurement of Doyle and Marruss,[24] and the β-decay studies[1] have defined the parity as negative. Strong population of the ground state by a direct (n, γ) transition, as observed in the present experiment, is entirely consistent with the $I^{\pi}=1^-$ assignment. The energy of the 63.6-keV level is defined as 63.583 ± 0.002 keV by an intense (n, γ) transition of this energy. The internal-conversion data[6] define the character of this transition as $M1$, which restricts the spin of the 63.6-keV level to 0, 1, or 2 with negative parity. The unique first-forbidden character[1] of the β transition from the ^{188}W ground state to this level defines the spin as $I^{\pi}=2^-$. This assignment is in agreement with the direct (n, γ) population of the 63.6-keV level, as observed in the present experiment. The established level at 156.0 keV is excited by both (n, γ) and (d, p) reactions. Low-energy (n, γ) transitions connect this level with the two lower states and define the energy of 156.047 ± 0.002 keV. The $M1$ character[6] of the 92.5-keV transition implies $I = 1$, 2, or 3 and negative parity for the 156.0-keV state. The very low intensity of the 156.0-keV crossover transition in comparison with the intense transition to the 63.6-keV state suggest $I^{\pi}=3^-$ as the most reasonable assignment.

2. Level at 169.4 keV

The 169.4-keV level, already well established to have $I^{\pi}=3^-$ by previous experiments, is populated by both the high-energy (n, γ) and (d, p) reactions. In addition to the established[1] depopulation to the 63.6-keV level, a weak 169.47-keV transition is observed which suggests depopulation of this level directly to the ground state.

3. Isomeric Level at 172.1 keV

Early investigations by Mihelich[25] and Flammersfeld[26] established the existence of a 19-min isomeric level in ^{188}Re. In a series of ingenious experiments which used a preaccelerating electric field in combination with a lens spectrometer, Takahashi, McKeown, and Scharff-Goldhaber[2] were able to identify the electron lines originating from the internal conversion of transitions which depopulate a state with energy 171.96 ± 0.13 keV to the levels at 156.0 and 169.4 keV. Measured M-subshell internal-conversion ratios[2] indicate that the 15.9-keV transition to the 156.0-keV state has $M3$ multipolarity. Thus the 172.1-keV isomer is assigned $I^{\pi}=6^-$.

The present measurements indicate that the 172.1-keV level is populated from a level at 360.883 keV. The observed transition energy of 188.813 keV connecting these levels establishes the energy of the isomer as 172.070 ± 0.008 keV.

4. Level at 182.8 keV

Both (n, γ) and (d, p) reactions indicate that a level exists near 182 keV. The high-energy (n, γ) data provide the more precise energy for the level, namely 182.76 ± 0.10 keV. Energy loops constructed using the low-energy capture γ rays fail to suggest an obvious mode of decay for a level at this approximate energy. The fact that γ transitions from this level to the ground and first excited states are not observed suggests that this level has high spin ($I \geq 4$) and decays via very low-energy transitions to the only available states of high spin, i.e., one or both of the $I^{\pi}=3^-$ states at 156.0 and 169.4 keV. This interpretation is strongly supported by the heretofore unexplained observations of BKL,[4] who observed in ^{188}Re delayed transitions ($T_{1/2}=7.7$ nsec) of energy 62 ± 3, 103 ± 6, and 166 ± 4 keV. These transitions could result from the decay of an isomeric level at 182 keV via an $\approx$13-keV transition to the 169.4-keV level.

In order to confirm that the delayed transitions reported by BKL[4] do indeed correspond to the known transitions which depopulate the 169.4-keV state, the delayed-coincidence measurements were repeated during the present study (see Sec. II E). Although the actual experimental situation appears to be considerably more complex than reported by BKL,[4] as there are at least five short-lived isomeric states in ^{188}Re, our original conclusions concerning the isomeric nature of the 182.7-keV level, based on the data of Ref. 4, were confirmed by the new measurements. In particular, the existence of a delayed transition ($T_{1/2}=17.6 \pm 3$ nsec) of energy 105.86 keV is interpreted as resulting from the isomeric character of the 182.7-keV level.

Although no transitions directly connecting a 182.7-keV state with *lower* states have been observed in the (n, γ) spectrum, there are several transitions which have the appropriate energy to connect a state at 182.744± 0.005 keV with well established higher-lying levels (see Fig. 7). Since this value of excitation energy is in excellent agreement with the high-energy (n, γ) value, the proposed identification is presumed to be correct and the corresponding γ-ray transitions have been assigned to the 182.7-keV state. In view of the direct (n, γ) population of this state and the absence of observable depopulation, as discussed above, the assignment $I = 4$ is suggested.

5. *Level at 205.3 keV*

Two low-energy γ-ray transitions to the ground and first excited states define the energy of a level at 205.342 ± 0.003 keV, which is populated by both (n, γ) and (d, p) reactions. The $M1$ character of the 141.8-keV transition to the 63.6-keV level and the absence of direct β-decay population of this state from ^{188}W suggest an assignment of $I^{\pi} = 2^-$. The stronger of the two depopulating transitions ($E_{\gamma} = 141.8$ keV) was observed to have a delayed component with $T_{1/2} = 3.2 \pm 0.6$ nsec. This lifetime has therefore been assigned to the 205.3-keV level.

6. *Level at 207.9 keV*

The coincidence data, an energy loop involving three transitions (92.355 + 207.849 ≅ 300.210 keV), and the established existence of a level at 300.2 keV, combine to suggest a level at 207.9 keV. The $E1$ multipolarity of the 207.9-keV transition to the ground state restricts the spin of this new level to $I^{\pi} = 0^+$, 1^+, or 2^+. Absence of direct (n, γ) population of the state and absence of an observable transition from it to the 2^- state at 63.6 keV both imply that $I^{\pi} = 0^+$ for the 207.9-keV level. The delayed-coincidence data of Sec. II E indicate that the 207.9-keV transition has a half-life of 3.2 ± 0.4 nsec, and it is therefore assumed that this is the half-life of the 207.9-keV state.

The existence of a positive-parity spin-zero level at 207 keV is consistent with all available experimental evidence, with a single exception: no such state was reported in previous studies of the β decay of ^{188}W. Examination of the γ-ray spectrum presented in Ref. 1 offered no hint of a 207-keV line which would indicate a β branch to the proposed $I^{\pi} = 0^+$ level. However, because of the close proximity of the expected 207.9-keV line to the intense 227.1-keV line which occurs in the ^{188}W decay and because of the experimental difficulties imposed by the necessity of frequent chemical purifications of the source to eliminate buildup of the ^{188}Re ground-state activity, with the attendant 155-keV line of ^{188}Os, a *weak* transition at 207 keV could have gone unresolved with the NaI detectors that were used in the experiments of Ref. 1. It appeared that a significant improvement in the sensitivity of detection of the 207-keV transition was possible using Ge(Li) detectors, and so the measurements described in Sec. II F were undertaken.

Successful observation of the β decay of ^{188}W to the 207.9-keV level is consistent with the hypothesized spin and parity assignment for this state.

7. *Levels at 230.9 and 256.9 keV*

Levels at 230.9 and 256.9 keV were first proposed by Suarez *et al.*[6] on the basis of low-energy γ-ray loops. The present work confirms the existence of both states. The 256.9-keV state is excited in the ^{187}Re(d, p) reaction, and both states are populated by high-energy capture γ-ray transitions. In addition, the coincidence data confirm the placement of several of the stronger transitions that originally suggested the existence of these levels. The spin assignments of the earlier work, namely $I^{\pi} = 2^+$, or 3^+ for the 230.9-keV state and $I^{\pi} = 2^-$ for the 256.9-keV state, remain unchanged. However, the delayed-coincidence measurements indicate that the 230.9-keV state has a lifetime of 20.9± 2 nsec (see Sec. II E).

8. *Levels at 284.6, 287.1, and 290.7 keV*

Both the high-energy (n, γ) and the (d, p) reaction data suggest the existence of one or more levels near 286 keV in addition to the established[1,2] $I^{\pi} = 1^-$ state at 290.7 keV. The high-energy (n, γ) results do not uniquely determine the energy of the states in the 285-keV region because of interference from the transition to the 290.7-keV level. However, the observed spectral shape is most consistent with a level at about 287 keV. On the other hand, the (d, p) data suggest, after allowing for the presence of the 290-keV proton group in the spectrum, a somewhat lower energy – approximately 284 keV.

It has been assumed, therefore, that there are two *new* levels near 285 keV. Energy loops formed from combinations of the low-energy γ rays support this interpretation and, in fact, define the energies of these two states as 284.600± 0.003 and 287.127± 0.005 keV. Since both of these states decay to $I^{\pi} = 3^-$ states via $M1$ transitions, their spins are restricted to $I = 2$, 3, or 4 with negative parity.

A note of caution is perhaps appropriate in regard to the use of energy loops to define new levels. The great number of low-energy transitions causes the occurrence of many purely accidental energy loops. It has been customary in the present work to use energy loops to define the existence of a new state only if some independent evidence for the occurrence of a state at that approximate energy was available – e.g. (n, γ), (d, p) or coincidence data.

9. Levels Above 300 keV

A large number of levels with energies greater than 300 keV are populated by the (d, p) and (n, γ) reactions. It has been possible to define the decay modes of almost all such levels that lie below ≈700 keV by using the low-energy γ rays of Table II together with the coincidence data. Computer routines, which scan the list of γ rays to identify transitions between known levels and which also suggest new levels based on energy sums, have been of considerable assistance in developing the level scheme. For most of the higher levels the available information is adequately presented by Fig. 7. The spin assignments shown in this figure have been made by utilizing the internal-conversion data of Ref. 6 (see Table II), with the additional assumption that γ-ray transitions of octupole and higher order will not be observed if dipole or quadrupole transitions are energetically permitted.

A few levels deserve some detailed comment since the reasoning employed in establishing the spin assignment is not immediately obvious, or in some cases, the evidence is contradictory. The 300.2-keV state decays to the $I^\pi=2^-$ state at 63.6 keV via a 236.6-keV $E1$ transition. The placement of this transition is confirmed by the coincidence data. On the basis of this $E1$ transition the spin of the 300.2-keV level is restricted to $I^\pi=1^+$, 2^+, or 3^+. However, Suarez et al.[6] also report that the 92.4-keV γ ray, which the coincidence data specify as connecting the 300.2-keV level with the $I^\pi=0^+$ state at 207.8 keV, has $E1$ character. This is inconsistent with the former parity assignment. Since the 92.4-keV line is not completely resolved in the work of Ref. 6, we have assumed that in reality this line has the next most reasonable multipolarity consistent with the measured conversion-electron intensity, namely $E2$. With this interpretation the 300.2-keV level is defined to have $I^\pi=2^+$.

A state at 335.7± 4 keV is excited in the (d, p) reaction. No corresponding state was observed in the (n, γ) work, nor was it possible to establish a more precise energy for the state by the identification of transitions to other levels. These facts suggest, but of course do not prove, that the level has high spin ($I \geq 5$).

B. Application of the Nilsson Model

In developing the level scheme we have attempted, up to this point, to make spin and parity assignments without specific reference to nuclear models. However, it will become apparent in the following section that application of the Nilsson model to the levels of ^{188}Re not only provides a rationale for the levels observed, but suggests extensions of the level scheme. To differentiate between those aspects of the level scheme which are model-independent and those aspects which are not uniquely determined by experiment we present in Figs. 8 and 9 a level scheme for ^{188}Re based on the Nilsson model. This should be compared with the level scheme presented in Fig. 7 and discussed in Sec. III A, which is independent of a specific model.

A reasonable experimental value of the deformation of ^{188}Re is $\epsilon=0.18$. This value, which is slightly higher than the figure 0.162 given by Löbner, Vetter, and Hönig,[27] is obtained from the same experimental data but with a heavier weighting of the half-life results. It is to be compared with the value of $\epsilon \simeq 0.20$ for ^{186}Re.[28,12] This change in deformation between ^{186}Re and ^{188}Re may be responsible for the fact that the neutron orbital for the ground-state configuration remains the same in both nuclei.

The Nilsson level density for neutrons is consid-

TABLE VII. Expected low-lying Nilsson configurations in ^{188}Re. The two rotational bands which arise from each configuration are listed in order of increasing energy according to the prediction of the Gallagher-Moszkowski coupling rule. The known experimental band-head energies are given in parentheses.

Proton	Neutron	K^π(lower)	K^π(higher)
$\frac{5}{2}^+[402\uparrow]$	$\frac{3}{2}^-[512\downarrow]$	1^- (0 keV)	4^- (183 keV)
	$\frac{1}{2}^-[510\uparrow]$	3^- (169 keV)	2^- (257 keV)
	$\frac{7}{2}^-[503\uparrow]$	6^- (172 keV)	1^- (291 keV)
	$\frac{9}{2}^-[505\downarrow]$	2^- (205 keV)	7^-
	$\frac{11}{2}^+[615\uparrow]$	8^+	3^+ (439 keV)
	$\frac{3}{2}^-[501\uparrow]$	4^- (325 keV)	1^- (557 keV)
$\frac{9}{2}^-[514\uparrow]$	$\frac{3}{2}^-[512\downarrow]$	3^+ (230 keV)	6^+
	$\frac{1}{2}^-[510\uparrow]$	5^+ (361 keV)	4^+
	$\frac{7}{2}^-[503\uparrow]$	8^+	1^+ (482 keV)
	$\frac{9}{2}^-[505\downarrow]$	0^+ (208 keV)	9^+
	$\frac{11}{2}^+[615\uparrow]$	10^-	1^-
	$\frac{3}{2}^-[501\uparrow]$	6^+	3^+

erably higher than that for protons in ^{188}Re.[29] The lowest-lying configurations which arise from the low-lying proton and neutron Nilsson orbitals are presented in Table VII. Each configuration gives rise to two intrinsic states, corresponding to parallel or antiparallel alignment of the spin-projection quantum numbers, i.e. $K=|\Omega_p \pm \Omega_n|$. The Gallagher-Moszkowski coupling rule[30] predicts the energy ordering of the two states, as indicated by K(lower) and K(higher) in Table VII. Those rotational bands which have been identified in the present work are also indicated in Table VII. In the following paragraphs, the configurations are discussed in order of increasing energy.

1. $\frac{5}{2}^+[402\uparrow] \pm \frac{3}{2}^-[512\downarrow]$ *Configuration*

The lowest-lying configuration in ^{188}Re has previously[1,2] been established as $\frac{5}{2}^+[402\uparrow] - \frac{3}{2}^-[512\downarrow]$. The first two rotational members of this $K^\pi = 1^-$ ground-state band are well established. This research determines their energies accurately as 63.582 and 156.047 keV. From these energies, the rotational formula

$$E = AI(I+1) + BI^2(I+1)^2 , \tag{1}$$

yields the parameters $A = 16.284$ keV and $B = -0.0485$ keV. These parameters in turn suggest 4^-, 5^-, and 6^- levels at 273.9, 412.5, and 566.0 keV, respectively. The γ-ray depopulation modes of the states at 287.1 and 448.2 keV suggest their assignment as the 4^- and 5^- members of the ground-state band (see Figs. 8 and 9). However, the experimental energies differ considerably from the values calculated above. These differences are reasonably explained qualitatively on the basis of a second-order Coriolis coupling with the $K=3^-$ band of the $\frac{5}{2}^+[402\uparrow] + \frac{1}{2}^-[510\uparrow]$ configuration. The inertial parameter, A, of this latter band is smaller than that of the ground-state band, and the 3^- band head lies just above the 3^- member of the ground-state band in such a way that the 4^- and 5^- members of the $K=3$ band lie *below* the 4^- and 5^- members of the ground-state band. Thus, the second-order Coriolis coupling lowers the energy of the 3^- member of the ground-state band while tending to raise the energies of the 4^- and 5^- members of the ground-state band, thereby giving poor agreement between experiment and the simple theory of Eq. (1). It seems probable that the mechanism of the mixing of the $K^\pi = 1^-$ (ground state) and $K^\pi = 3^-$ bands is largely via the 2^- band with the configuration $\frac{5}{2}^+[402\uparrow] - \frac{1}{2}^-[510\uparrow]$.

The above analysis suggests that the ground-state $K=1$ band in ^{188}Re must have $K^\pi = 2^-$ and $K^\pi = 3^-$ admixtures. This is clearly borne out in the γ decay of the 5^- and 4^- members of the band, which proceeds to states that are largely $K=3$ as well as to states that are predominantly $K=1$. Indeed, the relative intensities of these γ transitions are the primary data that allow the sorting out of the two sets of 3^-, 4^-, and 5^- states into their respective bands.

The parallel coupling of the $\frac{5}{2}^+[402\uparrow]$ and $\frac{3}{2}^-[512\downarrow]$ orbitals gives rise to a $K^\pi = 4^-$ band. The known $I=4$ level at 182.74 keV is an obvious candidate for the band head. The (d, p) cross section for this level is in good agreement with this interpretation. Figure 7 indicates that the 4^- band head decays by an ≈13-keV $M1$ transition to the 169.4-keV level (the band head of the $\frac{5}{2}^+[402\uparrow] + \frac{1}{2}^-[510\uparrow]$ configuration). The deduced γ-ray half-life of this transition, $T_{1/2\,\gamma} = 6.3 \times 10^{-6}$ sec corresponds to a retardation of ≈700 relative to the Weisskopf estimate (see Sec. III C). This is entirely consistent with the retardation factors for similar $M1$ transitions compiled by Löbner.[31]

The A value of the $K^\pi = 1^-$ band of this configuration suggests that the first rotational member of the $K^\pi = 4^-$ band should lie at ≈340 keV. A 5^- state will not be observably populated by a direct (n, γ) transition. However, a state with the appropriate (d, p) cross section is observed at 335.7± 4 keV. Such a state should decay to the 4^- band head and perhaps also to the 6^- band head at 172.070 keV. Unfortunately no *unique* set of low-energy γ rays allows the accurate definition of the energy of this state.

2. $\frac{5}{2}^+[402\uparrow] \pm \frac{1}{2}^-[510\uparrow]$ *Configuration*

The 3^- state at 169.4 keV has previously[1] been assigned as the $K^\pi = 3^-$ band head of the configuration $\frac{5}{2}^+[402\uparrow] + \frac{1}{2}^-[510\uparrow]$. The experimental (d, p) cross section is consistent with this interpretation. The observed γ-ray decay and (d, p) cross section of the 284.6-keV level suggests this state as the $I^\pi = 4^-$ member of the $K=3$ band. An additional level at 429.8 keV which is apparently populated in the (d, p) reaction has been tentatively assigned as the $I^\pi = 5^-$ rotational band member. The observed γ decay of these levels further suggests the mixed nature of this band, as discussed in Sec. III B 1. The rotational band parameters are given in Table VIII.

The antiparallel coupling of the $\frac{5}{2}^+[402\uparrow] \pm \frac{1}{2}^-[510\uparrow]$ configuration gives rise to a $K^\pi = 2^-$ band, which we have identified with the $I^\pi = 2^-$ state at 256.9 keV. This identification is suggested primarily by the existence of a strong transition between this 2^- state and the $K^\pi = 3^-$ band head at 169.4 keV. The γ-ray decay mode of the states at 372.1 and 523.0 keV suggests that these levels are the 3^- and 4^- rotational states of this $K=2$ band. The relative (d, p) cross sections are consistent with these assignments. However it should be noted that all the states which involve the $\frac{1}{2}^-[510\uparrow]$ neutron configuration seem to have systematically larger (d, p) cross sections than that suggested by theory (see Table XII). As expected, the majority of the low-energy γ-ray transition strength from the higher states in both the $K^\pi = 2^-$ and $K^\pi = 3^-$ bands tends to stay within the bands. However, depopulating transitions from both bands show evidence of the Coriolis mixing of these bands with each other and with the ground-state band.

3. $\frac{5}{2}^+[402\uparrow] \pm \frac{7}{2}^-[503\uparrow]$ *Configuration*

The 6^- state at 172.1 keV has previously[1,2] been assigned as the $K^\pi = 6^-$ band head of the configuration $\frac{5}{2}^+[402\uparrow] \pm \frac{7}{2}^-[503\uparrow]$. A very intense proton group observed at 169.8 keV in the (d, p) reaction (assumed in this interpretation to be an unresolved doublet) is consistent with this assignment. Rotational states built on this band head are predicted to have very small (d, p) cross sections, and in fact no evidence of such rotational states has been found.

TABLE VIII. Rotational band parameters.

Configuration	K^π	Band head energy (keV)	A (keV)	B (keV)
$\frac{5}{2}^+[402\uparrow] - \frac{3}{2}^-[512\downarrow]$	1^-	0.0	16.28	−0.048
$\frac{5}{2}^+[402\uparrow] + \frac{1}{2}^-[510\uparrow]$	3^-	169.44	14.18	+0.007
$\frac{5}{2}^+[402\uparrow] + \frac{7}{2}^-[503\uparrow]$	6^-	172.07		
$\frac{5}{2}^+[402\uparrow] + \frac{3}{2}^-[512\downarrow]$	4^-	182.76	~15.3	a
$\frac{5}{2}^+[402\uparrow] - \frac{9}{2}^-[505\downarrow]$	2^-	205.34	19.18	−0.032
$\frac{9}{2}^-[514\uparrow] - \frac{9}{2}^-[505\downarrow]$	0^+	207.85	15.48	−0.014
$\frac{9}{2}^-[514\uparrow] - \frac{3}{2}^-[512\downarrow]$	3^+	230.91	15.19	a
$\frac{5}{2}^+[402\uparrow] - \frac{1}{2}^-[510\uparrow]$	2^-	256.92	19.61	−0.023
$\frac{5}{2}^+[402\uparrow] - \frac{7}{2}^-[503\uparrow]$	1^-	290.67	18.10	−0.011
$\frac{5}{2}^+[402\uparrow] + \frac{3}{2}^-[501\uparrow]$	4^-	325.87		
$\frac{9}{2}^-[514\uparrow] - \frac{9}{2}^-[505\downarrow]$	0^+	346.57	15.32	a
$\frac{9}{2}^-[514\uparrow] + \frac{1}{2}^-[510\uparrow]$	5^+	360.88	15.78	a
$\frac{5}{2}^+[402\uparrow] - \frac{11}{2}^+[615\uparrow]$	3^+	439.75	16.96	a
$\frac{9}{2}^-[514\uparrow] - \frac{7}{2}^-[503\uparrow]$	1^+	482.16	15.10	−0.032
$\frac{5}{2}^+[402\uparrow] - \frac{3}{2}^-[501\uparrow]$ [b]	1^-	556.83	14.03	−0.121
$\frac{5}{2}^+[402\uparrow] - \frac{3}{2}^-[501\uparrow]$ [b]	1^-	582.16	16.26	+0.003

[a] Insufficient members of the band are observed to calculate B, which is assumed to be zero in calculating A.

[b] These bands involve both intrinsic and $|K-2|$ γ-vibrational components (see text).

The antiparallel coupling of this configuration gives rise to a $K^\pi = 1^-$ band, the lowest two states of which have been previously[1,2] assigned at 290.7 and 362.7 keV. The rotational energy sequence suggests that the state at 470.1 keV is the $I^\pi = 3^-$ member of this band. These assignments are supported by the experimental (d,p) cross sections. It has been pointed out in Ref. 1 that the branching ratio of the γ-ray transitions from the $K^\pi = 1^-$ band at 290.7 keV to the lowest two members of the ground-state rotational band are in excellent agreement with the simple branching-ratio prediction of Alaga.[32] However in view of the fact that the major Nilsson orbital components of these states do not allow an $M1$ transition, it appears that such agreement is fortuitous. We have attempted to apply the Alaga rules for other transition probability ratios (where the simple rules should apply) with varying success. We suspect that, in general, Coriolis coupling induces sufficient K mixing that the Alaga rules do not apply.

4. $\frac{5}{2}^+[402\uparrow] \pm \frac{9}{2}^-[505\uparrow]$ *Configuration*

The systematics of the Nilsson orbitals[29] indicate that a configuration involving the $\frac{9}{2}^-[505\uparrow]$ neutron orbital is expected in the low-lying spectrum. The antiparallel coupling of the $\frac{5}{2}^+[402\uparrow] - \frac{9}{2}^-[505\uparrow]$ configuration, with $K^\pi = 2^-$, is expected to be the lower lying of the two bands of this configuration. The weakly (d,p)-populated 2^- state at 205.3 keV is assigned as this band head. Not only is the experimental (d,p) cross section in good agreement with the value calculated for this band head, but also the observed retardation factors for the two $M1$ transitions connecting this state with the ground-state band strongly support this assignment. The experimental data indicate the existence of two negative-parity states at 316.9 and 462.1 keV. The (d,p) cross sections and the rotational systematics suggest that these states are the 3^- and 4^- rotational members of the $K^\pi = 2^-$ band.

The $K^\pi = 7^-$ band that corresponds to the parallel coupling of these Nilsson orbitals is not observed, presumably because of the difficulty of detecting a state of such a high spin unless it is an isomer.

5. $\frac{9}{2}^-[514\uparrow] \pm \frac{3}{2}^-[512\downarrow]$ *Configuration*

The $\frac{9}{2}^-[514\uparrow]$ orbital is expected to be the lowest-lying excited proton configuration in ^{188}Re. This Nilsson orbital, which lies below the Fermi level, occurs at 387 keV in ^{185}Re and 206 keV in ^{187}Re (see Ref. 29). Thus one expects to observe the $K^\pi = 3^+$ band head arising from the antiparallel coupling of this orbital and the $\frac{3}{2}^-[512\downarrow]$ neutron orbital somewhat below the average of 206 and

387 keV. The 2^+ or 3^+ state observed at 230.91 keV fits the requirements for the band head. It should be noted that pure excited proton configurations are not expected to be populated in the (d,p) reaction. The retardation ($F_W \approx 10^5 - 10^6$) of the two K-forbidden $E1$ transitions is consistent with the proposed assignment. The state observed at 352.4 keV has the correct properties to be the 4^+ first rotational member of the $K^\pi = 3^+$ band. Not only is the moment of inertia appropriate, but this state depopulates to the band head and to the accessible 3^- states.

The parallel coupling of this configuration gives rise to a $K^\pi = 6^+$ band. No evidence of such a band has resulted from the present work, presumably for reasons analogous to those presented in Sec. C 4.

6. $\frac{9}{2}^-[514\uparrow] + \frac{1}{2}^-[510\uparrow]$ Configuration

A state with 5.2-nsec half-life and spin 5^+ is observed at 360.9 keV. This state decays via an enhanced $E2$ transition (see Table IX) to the 3^+ band head of the configuration $\frac{9}{2}^-[514\uparrow] - \frac{3}{2}^-[512\downarrow]$. In view of this enhanced $E2$ and the Coriolis mixing expected between the $\frac{1}{2}^-[501\uparrow]$ and $\frac{3}{2}^-[512\downarrow]$ neutron configurations, the $\frac{9}{2}^-[514\uparrow] + \frac{1}{2}^-[510\uparrow]$ configuration is the most reasonable assignment for this state. The retarded $E1$'s ($F_W \approx 10^5$–10^6) depopulating to the 4^- and 6^- band heads at 182.7 and 172.1 keV, respectively, are also consistent with this assignment. The coincidence data suggest a possible location for the 6^+ first rotational member of this $K^\pi = 5^+$ band at 550.2 keV.

The antiparallel coupling of this configuration gives rise to a $K^\pi = 4^+$ band which is expected to lie above the $K^\pi = 5^+$ band. We find no experimental evidence for this band.

7. $\frac{9}{2}^-[514\uparrow] - \frac{9}{2}^-[505\downarrow]$ Configuration

A 0^+ state with $T_{1/2} = 3.2$ nsec is observed at 207.8 keV. In view of the available Nilsson orbitals (see Table VII), the only reasonable assignment for such a state is $\frac{9}{2}^-[514\uparrow] - \frac{9}{2}^-[505\downarrow]$. The large retardation of the $E1$ transition from this state to the ground state (see Table IX) is explained by the fact that both neutron and proton configurations differ from those of the ground state. The observation of a $K^\pi = 0^+$ band is of particular theoretical interest because of the expected shift between the even- and odd-spin members of such a band (see Sec. III F). Obvious candidates for additional members of this band are the 2^+ state at 300.213 and the 1^+ state at 346.6 keV. Not only is the moment of inertia implied by the 0^+-2^+ energy spacing reasonable, but also the strong intraband transitions suggest these assignments. The energies of the lowest three levels of this $K^\pi = 0^+$ band suggest that the 3^+ member should occur at approximately 500 keV. The state observed at 499.7 keV with $K^\pi = (1^+, 2^+, 3^+)$ decays within the band and is therefore presumed to be the 3^+ member. In a similar manner we identify the state at 511.7 keV as the 4^+ member of this band. Using the five assigned members of this $K = 0$ band, it is possible to calculate separate values of A for the odd and even members. As expected, these values are very nearly equal (see Table VIII). In addition, it is possible to deter-

TABLE IX. Delayed transitions.

Level (keV)	$T_{1/2}$(exp) of level	Transition energy (keV)	Initial state	Final state	Multipolarity	$T_{1/2\gamma}$(exp)	ΔK	F_W
172.07	18.7 min	2.63	$\frac{5}{2}^+[402] + \frac{7}{2}^-[503]$	$\frac{5}{2}^+[402] + \frac{1}{2}^-[510]$	$M3$	2.6×10^{15} sec [a]	3	37 [a]
		16.03	$\frac{5}{2}^+[402] + \frac{7}{2}^-[503]$	$\frac{5}{2}^+[402] - \frac{3}{2}^-[512]$	$M3$	5.0×10^{10} sec	5	221
182.76	17.6 nsec	13.30	$\frac{5}{2}^+[402] + \frac{3}{2}^-[512]$	$\frac{5}{2}^+[402] + \frac{1}{2}^-[510]$	$M1$	6.3 μsec	1	663
205.34	3.2 nsec	141.76	$\frac{5}{2}^+[402] - \frac{9}{2}^-[505]$	$\frac{5}{2}^+[402] + \frac{3}{2}^-[512]$	$M1$	10.8 nsec	1	1350
		205.35	$\frac{5}{2}^+[402] - \frac{9}{2}^-[505]$	$\frac{5}{2}^+[402] + \frac{3}{2}^-[512]$	$M1$	28.6 nsec	1	1.1×10^4
207.84	3.2 nsec	207.85	$\frac{9}{2}^-[514] - \frac{9}{2}^-[505]$	$\frac{5}{2}^+[402] - \frac{3}{2}^-[512]$	$E1$	3.41 nsec	1	1.49×10^5
230.91	21 nsec	74.86	$\frac{9}{2}^-[514] - \frac{3}{2}^-[512]$	$\frac{5}{2}^+[402] - \frac{3}{2}^-[512]$	$E1$	62.5 nsec	2	1.28×10^5
		167.3	$\frac{9}{2}^-[514] - \frac{3}{2}^-[512]$	$\frac{5}{2}^+[402] - \frac{3}{2}^-[512]$	$E1$	56.1 nsec	2	1.42×10^6
360.89	5.25 nsec	129.98	$\frac{9}{2}^-[514] + \frac{1}{2}^-[510]$	$\frac{9}{2}^-[514] - \frac{3}{2}^-[512]$	$E2$	87.8 nsec	2	0.37
		178.13	$\frac{9}{2}^-[514] + \frac{1}{2}^-[510]$	$\frac{5}{2}^+[402] + \frac{3}{2}^-[512]$	$E1$	30.7 nsec	1	8.8×10^5
		188.81	$\frac{9}{2}^-[514] + \frac{1}{2}^-[510]$	$\frac{5}{2}^+[402] + \frac{7}{2}^-[503]$	$E1$	7.8 nsec	1	2.6×10^5

[a] Based on an estimated total internal-conversion coefficient of 1.34×10^{12}.

mine the splitting energy between the even and odd members, which can be usefully compared with theory. This comparison, which is important in evaluating the neutron-proton force, is discussed separately in Sec. III F. Because of the high spin, the band which results from the parallel coupling of this configuration was not observed.

8. $\frac{5}{2}^+[402\uparrow] - \frac{11}{2}^+[615\uparrow]$ *Configuration*

The $\frac{5}{2}^+[402\uparrow] \pm \frac{11}{2}^+[615\uparrow]$ configuration will give rise to $K^\pi = 8^+$ and 3^+ bands. According to the Gallagher-Moszkowski coupling rules, the $K^\pi = 8^+$ band should be the lower lying of the two. Since it has not been observed as an isomer in ^{188}Re, we assume that this state lies above the known $K^\pi = 6^-$ isomer at 172.1 keV. No experimental evidence of its existence has been obtained. The most reasonable candidate for the $I^\pi = 3^+$ band head is a state at 439.8 keV, with known $I^\pi = (2^+, 3^+)$. This state decays as expected to the 2^- band head of the $\frac{5}{2}^+[402\uparrow] - \frac{9}{2}^-[505\downarrow]$ configuration. The strong transition which connects the 439.8-keV state with the other $K^\pi = 3^+$ band head is not easily understood in view of the fact that both the neutron and proton configurations of these two states are different. However, the existence of this transition may suggest that some other interaction (such as a neutron-proton force) is mixing these states of identical $I^\pi K$. The state at 575.4 keV, which depopulates to the band head and to the 3^- member of the $\frac{5}{2}^+[402\uparrow] - \frac{9}{2}^-[505\downarrow]$ configuration, can reasonably be assigned as the 4^+ first rotational member of this band. Interestingly, this state also decays to the other state with $I^\pi K = 4^+3$, as observed for the band head.

9. $\frac{9}{2}^-[514\uparrow] - \frac{7}{2}^-[503\uparrow]$ *Configuration*

A positive-parity state with $I = 1$ or 2 is observed at 482.2 keV. No reasonable combination of Nilsson neutron and proton configurations can lead to a 2^+ band head in this energy region. A $K^\pi = 2^+$ band head can, however, arise as the γ vibration built on the 207.8-keV $K^\pi = 0^+$ band. This alternative seems to be excluded by the extremely low γ-vibrational energy which it implies ($\omega_{\gamma\,\mathrm{vib}} \cong 275$ keV). For example in the isobaric ^{188}Os nucleus, $\omega_{\gamma\,\mathrm{vib}} = 633$ keV. Although it is possible that an $I^\pi = 2^+$ state at this energy is a rotational member of a $K^\pi = 0^+$ or 1^+ band, no other evidence for such a band has been found. On the other hand if the state at 482.2 keV is assumed to be a $K^\pi = 1^+$ band head, rotational members can be identified at 541.6 and 628.9 keV. Such a $K^\pi = 1^+$ band has a very reasonable interpretation in terms of the Nilsson configuration $\frac{9}{2}^-[514\uparrow] - \frac{7}{2}^-[503\uparrow]$. This interpretation is suggested not only by the observed energy systematics of the band but also by the observed γ-decay characteristics of these states.

10. $\frac{5}{2}^+[402\uparrow] \pm \frac{3}{2}^-[501\uparrow]$ *Configuration*

The largest theoretical (d,p) cross section populating levels in ^{188}Re is predicted for the $I^\pi K = 4^-4$ band head of the $\frac{5}{2}^+[402\uparrow] + \frac{3}{2}^-[501\uparrow]$ configuration. The level at 325.9 keV is identified as this state since it is intensely populated in the (d,p) reaction. As expected, this state depopulates primarily to the $K^\pi = 3^-$ and 4^- band heads at 169.4 and 182.8 keV. The weak transition to the 3^- state at 156.0 keV is interpreted as further evidence for $K = 3$ admixture in the ground-state band. No evidence for higher rotational members has been found, presumably because of the high spin and the extraordinarily small (d,p) cross sections of these states (see Table XII).

The antiparallel coupling of this configuration will give rise to a $K^\pi = 1^-$ band. Additional $K^\pi = 1^-$ bands in the neighborhood of 600 keV are expected to arise from both the $\frac{1}{2}^+[400\uparrow] - \frac{3}{2}^-[512\downarrow]$ configuration and from the $|K-2|$ γ vibration built on the ground state. Indeed, if these bands occur in the same energy region, they should be considerably mixed with the $K^\pi = 1^-$ band from the $\frac{5}{2}^+[402\uparrow] - \frac{3}{2}^-[401\uparrow]$ configuration. Two separate $K^\pi = 1^-$ bands can be constructed from the (n,γ) and (d,p) populated states, namely 556.8, 609.0, 680.1 keV and 582.2, 647.3, and 745.2 keV. The relative (d,p) cross sections of the two bands suggest that the 556.8-keV band has the larger $\frac{5}{2}^+[402\uparrow]$ proton component, while the 582.2-keV band has the larger vibrational or excited proton component. Significantly, the summed cross sections for the 1^-, 2^-, and 3^- members of these two bands are approximately those predicted for the $\frac{5}{2}^+[402\uparrow] - \frac{3}{2}^-[501\uparrow]$ configuration.

11. *Systematics of the Nilsson Configurations*

In this study, 15 rotational bands involving 41 states have been assigned to 10 Nilsson configurations. The energy systematics of the excited proton and neutron configurations, as assigned in the preceding paragraphs, is qualitatively consistent with the systematics of Nilsson states in the neighboring odd-A nuclei.[29] The energy (207.9 keV) of the 0^+ band head may appear to be an exception to this general consistency. A cursory inspection of Table VII would suggest that the 0^+ band head should occur at roughly 400 keV. However, both the odd-even shift and, more importantly, the absence of zero-point rotational energy for this band tend to reduce its excitation energy. In view of these factors the observed position of the band is not considered to be inconsistent with the energies of the other bands.

The calculated (d,p) cross sections are in remarkably good agreement with experiment, as shown in Fig. 10. The agreement between experiment and the Nilsson model is significant because $A=188$ is very near the boundary of the deformed nuclei, where departure from the simple theory might be expected.

In all cases where both parallel and antiparallel couplings of the neutron and proton configurations are observed, the ordering of the bands is correctly predicted by the Gallagher-Moszkowski rule. A quantitative discussion of the energy splittings between the band heads resulting from the two couplings is given in Sec. III F.

C. Measured Lifetimes

The experimental discussion of Sec. II E presents lifetime data on five low-lying states in ^{188}Re. The lifetime of a sixth state, the well-studied isomer at 172.0 keV, is known from earlier work.[2] It is useful to compare the γ-ray transition probabilities associated with these states with other known transition probabilities of deformed nuclei.

The experimental systematics of γ-ray transition probabilities has been summarized by Löbner.[31] In discussing lifetimes it is useful to calculate the Weisskopf hindrance factor, defined by:

$$F_W=\frac{T_{1/2\,\gamma}(\text{experiment})}{T_{1/2\,\gamma}(\text{Weisskopf estimate})}\,.$$

This parameter is listed for each measured transition in Table IX. Löbner's compilation indicates that values of F_W vary over a wide range, even for a given degree of K forbiddenness. Values differing by 3 orders of magnitude or more are found. This situation is not unexpected since transitions between the principal Nilsson components of the nuclear states involved are frequently forbidden. In such cases, the transition probability is dominated by admixtures whose amplitudes can differ widely for different states.

The 11 values of F_W presented in Table IX all lie within the range of values reported by Löbner for transitions of the appropriate multipolarity and ΔK. A more meaningful comparison of transitions in odd-odd nuclei could be made using $\Delta\Omega$, rather than ΔK, as a parameter. Unfortunately, no such summary of the available data has yet been published. The most highly retarded transitions are expected between states that do not mix via the Coriolis interaction with configurations which support allowed transitions. Such a case is the decay of the 205.3-keV level to the ground-state band. $M1$ transitions between the $\frac{9}{2}^-[505\downarrow]$ neutron configuration and the $\frac{3}{2}^-[512\downarrow]$ configuration of the ground-state band are Ω forbidden, as are transitions between other nearby Nilsson components which can be Coriolis-mixed with these configurations. The experimental data on the decay of the 205.3-keV state confirm this expected forbiddenness: The values $F_W\approx10^3-10^4$ lie near the high end of the range for known $M1$ transitions.[31]

Similar general arguments can be advanced to explain other values given in Table IX; however, detailed knowledge of the nuclear wave functions is necessary to propose a quantitative explanation of the measured quantities.

D. β Decay

The β decay of ^{188}W is for the most part directly understood in terms of the usual β-decay syste-

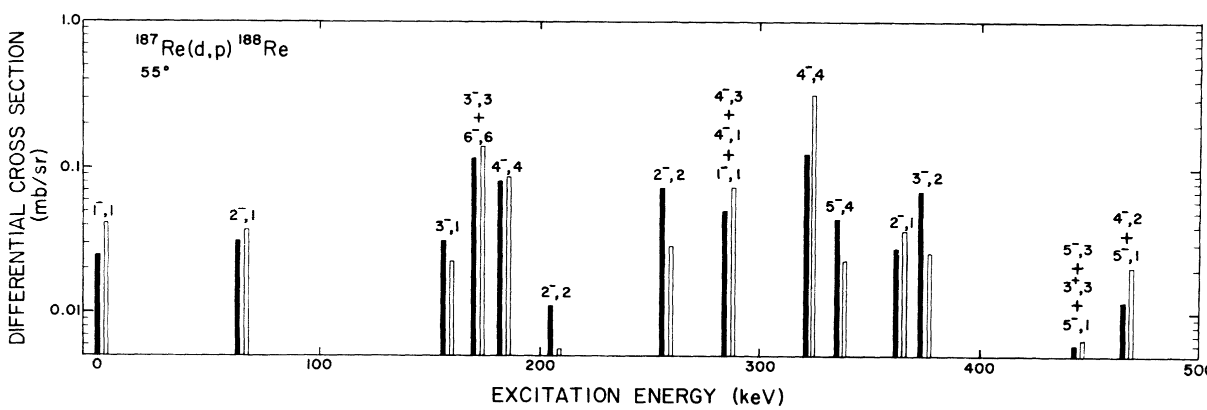

FIG. 10. Comparison of the experimental (solid bar) and theoretical (open bar) cross sections for the reaction ^{187}Re$(d,p)^{188}$Re at 55°.

matics and the Nilsson model. In particular, $\log ft$ values of 7.2 and 6.9 are reasonable for β_1 and β_5 (see Fig. 6), the transitions from the complex 0^+ ^{188}W ground state to the $1^-(\frac{5}{2}^+[402\uparrow]-\frac{3}{2}^-[512\downarrow])$ ground state and $1^-(\frac{5}{2}^+[402\uparrow]-\frac{7}{2}^-[503\uparrow])$, 290.7-keV state of ^{188}Re. Each of these transitions is a first-forbidden unhindered decay. Similarly, the unique first-forbidden transition to the 2^- first rotational band member built on the ground state might reasonably be expected to be forbidden by a factor of 100–1000 with respect to the transition to the ground state. The $\log ft$ of 9.8 for β_2 confirms this expectation. As expected in view of its second-forbidden nature, no observable β decay to the 3^- second rotational member of the ground-state band occurs.

A limit of $\log ft > 10.6$ has been set on the first-forbidden unique transition to the 2^- band head with the configuration $\frac{5}{2}^+[402\uparrow]-\frac{9}{2}^-[505\downarrow]$. Since the single-particle transition $\nu\frac{9}{2}^-[505\downarrow]\rightarrow\pi\frac{5}{2}^+[402\uparrow]$ is unique first-forbidden *hindered*, the higher $\log ft$ is not surprising.

The $0^+\rightarrow 0^+$ β transition between the ^{188}W ground state and the $0^+(\frac{9}{2}^-[514\uparrow]-\frac{9}{2}^-[505\downarrow])$ 207.8-keV state in ^{188}Re is of special interest. Allowed β transitions of $0^+\rightarrow 0^+$ type are pure Fermi transitions. However, Fermi matrix elements can act only between isobaric pairs in which the transitions have $\Delta T=0$. Among the light nuclei ($A\leq 56$) superallowed transitions of this type are commonly observed between low-lying states, with $\log ft$ values of ≈ 3.5. However, for heavier nuclei in which $N>Z$, the Fermi strength is concentrated in an isobaric analog state, which lies high in the spectrum and is usually energetically unavailable in β decay. Therefore $0^+\rightarrow 0^+$ transitions are highly forbidden.

Recently Damgaard[33] has been able to calculate $\log ft$ values for $0^+\rightarrow 0^+$ transitions in deformed rare-earth and actinide nuclei by mixing the isobaric analog states into the appropriate states involved in the decay. Typically, his $\log ft$ values fall in the range 8–10. Thus the $\log ft$ of 9.9 observed in the decay of ^{188}W is appropriate for this $0^+\rightarrow 0^+$ β transition. Indeed, this $\log ft$ value may be used to infer the amount of $T_Z=-20$ in the predominantly $T_Z=-19$, 0^+ state at 207.8 keV in ^{188}Re.

E. Calculation of (d, p) Cross Sections

The differential cross section for a deuteron stripping reaction on a target with total angular momentum I_i may be written as[34]

$$\frac{d\sigma}{d\Omega}=\frac{2I_f+1}{2I_i+1}\sum_{j,l}S_{j,l}\Phi_{l,j}(\theta)\,, \qquad (2)$$

where I_f is the total angular momentum of the final state; l and j are the orbital and total angular momenta, respectively, of the captured neutron; $S_{j,l}$ is the spectroscopic factor which expresses the overlap between the initial target state plus one neutron and the final nuclear state; and $\Phi_{l,j}(\theta)$ is the intrinsic single-particle cross section. In principle the spectroscopic factor is derivable from nuclear-structure theory and is therefore model-dependent. In these calculations the form of $S_{j,l}$ is that derived from the Nilsson model of two nucleons strongly coupled to a deformed core. The equations which express the spectroscopic factor in terms of the parameters of this model are given in Ref. 12.

For the reaction ^{187}Re$(d,p)^{188}$Re, the intrinsic single-particle cross sections have been evaluated for values of j which include all transferred angular momenta between $0\leq l\leq 6$. The calculations were made using the distorted-wave Born-approximation (DWBA) code DWUCK[35] with the optical-model parameters[36] given in Table X. If $\sigma_{l,j}$ is the (d,p) single-particle cross-section output by DWUCK, then the quantity $\Phi_{l,j}$ in Eq. (2) is given by

$$\Phi_{l,j}=N\sigma_{l,j}/(2j+1)\,,$$

where N is a normalization factor and has the value 1.53. The $\sigma_{l,j}$ values were determined for an incident deuteron energy of 12 MeV and a Q value corresponding to an excitation energy of 200 keV in ^{188}Re. No lower-cutoff radius was used in the DWBA analysis.

The $C_{j,l}$ coefficients required for evaluating the spectroscopic factors are given in Table XI and were obtained for a deformation $\epsilon=0.18$ from a computer code using a Woods-Saxon potential.[37] The occupation probabilities (U^2) for the relevant neutron configurations in ^{188}Re are also indicated. Table XII summarizes the calculated (d,p) cross sections for the six neutron configurations which have been considered. Results are given for reaction angles of 55 and 116°. A comparison between the experimental (d,p) cross sections and

TABLE X. Optical-model parameters used to compute the single-particle cross sections for the reaction ^{187}Re$(d,p)^{188}$Re.

	V (MeV)	r_0 (F)	A (F)	W_D (MeV)	r_I (F)	a_I (F)	V_{LS} [a] (MeV)
Deuteron	116.7	1.15	0.810	50.8	1.36	0.851	0.0
Proton	53.1	1.25	0.650	40.8	1.25	0.760	8.0
Bound state		1.25	0.650				7.5

[a] The usual λ factor describing the Thomas spin-orbit term is related to V_{LS} through $V\lambda=181.8\ V_{LS}$ and has a value of about 25 for protons and neutrons.

TABLE XI. $C^{\Omega}_{j,l}$ coefficients for the neutron orbitals in ^{188}Re for a deformation $\epsilon=0.18$.

U^2		[512↓] 0.50	[510↑] 0.25	[503↑] 0.76	[505↓] 0.78	[501↑] 0.84		[615↑] 0.875
j	l	$C^{3/2}_{j,l}$	$C^{1/2}_{j,l}$	$C^{7/2}_{j,l}$	$C^{9/2}_{j,l}$	$C^{3/2}_{j,l}$	l	$C^{11/2}_{j,l}$
$\frac{1}{2}$	1		+0.0903				0	
$\frac{3}{2}$	1	−0.4997	+0.6461			+0.7812	2	
$\frac{5}{2}$	3	+0.7054	+0.5560			+0.5481	2	
$\frac{7}{2}$	3	+0.3364	−0.3691	+0 .9342		−0.2080	4	
$\frac{9}{2}$	5	−0.3629	−0.3477	+0 .3298	+0.9967	−0.2117	4	
$\frac{11}{2}$	5	−0.0891	+0.0899	−0.1362	+0.0818	+0.0358	6	−0.0603
$\frac{13}{2}$							6	+0.9981

the theoretical values corresponding to the proposed configurational assignments indicates very satisfactory agreement (see Fig. 10 and Table XIII).

F. Calculation of the Splitting Energies of Gallagher-Moszkowski Pairs and the $K=0$ Odd-Even Shift

One of the important uses of the spectroscopy of odd-odd deformed nuclei is the study of the neutron-proton interaction. In ^{188}Re the splitting energies,

$$\Delta E = E_{K=\Omega_p+\Omega_n} - E_{K=|\Omega_p-\Omega_n|},$$

between the parallel and antiparallel couplings of four different configurations have been observed. After zero-point rotational energies are subtracted these experimental splitting energies can be

TABLE XII. Calculated (d,p) cross sections. Values are given in units of μb/sr. Cross sections which are appreciably less than 1 μb/sr have been omitted (· · ·).

Nilsson state Proton	Nilsson state Neutron	U^2	Coupling	θ (deg)	$I=0$	1	2	3	4	5	6	7	8
$\frac{5}{2}^+$[402↑]	$\frac{3}{2}^-$[512↓]	0.5	↑↑	55					90	20	3.0	· · ·	
				116					29	10	2.0	· · ·	
			↑↓	55		41	38	23	9.0	2.5	· · ·		
				116		12	13	9.5	4.5	1.5	· · ·		
$\frac{5}{2}^+$[402↑]	$\frac{1}{2}^-$[510↑]	0.25	↑↑	55				42	30	4.2	1.0	· · ·	
				116				13	10	2.5	· · ·		
			↑↓	55			32	31	12	2.5	· · ·		
				116			9.2	10	4.5	1.2			
$\frac{5}{2}^+$[402↑]	$\frac{7}{2}^-$[503↑]	0.76	↑↑	55							106	0.7	· · ·
				116							55	0.7	· · ·
			↑↓	55		40	37	21	7.6	1.5	· · ·		
				116		20	19	11	3.8	0.7	· · ·		
$\frac{5}{2}^+$[402↑]	$\frac{9}{2}^-$[505↓]	0.78	↑↑	55								9.3	0.8
				116								8.6	0.7
			↑↓	55			4.7	3.1	1.6	· · ·			
				116			4.1	2.6	1.2	· · ·			
$\frac{5}{2}^+$[402↑]	$\frac{3}{2}^-$[501↑]	0.84	↑↑	55					315	19	2.0	· · ·	
				116					93	9.3	1.1	· · ·	
			↑↓	55		154	118	50	12	1.7	· · ·		
				116		45	38	17	4.9	0.9	· · ·		
$\frac{5}{2}^+$[402↑]	$\frac{11}{2}^+$[615↑]	0.87	↑↑	55									1.1
				116									2.7
			↑↓	55				· · ·	1.6	1.5	0.6	· · ·	
				116				· · ·	3.9	3.6	1.7	· · ·	

TABLE XIII. Comparison of calculated and experimental splitting energies of Gallagher-Moszkowski pairs and the odd-even shift for ^{186}Re and ^{188}Re.

	Configuration		K^{π}		Theory	Experiment[a] (keV)	
	Proton	Neutron	$\sum_n + \sum_p = 0$	$\sum_n + \sum_p = 1$	(keV)	^{186}Re	^{188}Re
Parallel-antiparallel splitting	$\frac{5}{2}^+[402\uparrow]$	$\frac{3}{2}^-[512\downarrow]$	4^-	1^-	−131.8	−129.7	−137.4
	$\frac{5}{2}^+[402\uparrow]$	$\frac{1}{2}^-[510\uparrow]$	2^-	3^-	95.6	139.5	92.3
	$\frac{5}{2}^+[402\uparrow]$	$\frac{7}{2}^-[503\uparrow]$	6^-	1^-	238.4	207.9	208.7
	$\frac{5}{2}^+[402\uparrow]$	$\frac{3}{2}^-[501\uparrow]$	1^-	4^-	223.6	⋯	270.1
	$\frac{5}{2}^+[402\uparrow]$	$\frac{11}{2}^+[615\uparrow]$	3^+	8^+	144.0	238[b]	⋯
Odd-even shift	$\frac{9}{2}^-[514\uparrow]$	$\frac{9}{2}^-[505\downarrow]$			−60.1	⋯	−54.0

[a] The experimental splitting energies have been corrected for zero-point rotational energy by the addition of a term $\Delta E_{zp} = \bar{A}(K_{|\Omega_p - \Omega_n|} - K_{\Omega_p + \Omega_n})$, where $\bar{A}$ is the mean inertial parameter of the two bands.

[b] D. W. Seegmiller, M. Lindner, and R. A. Meyer, Nucl. Phys. A185, 94 (1972); the ground-state inertial parameter was used to calculate ΔE_{zp}.

compared with theoretical calculations of this splitting determined by the form of the residual neutron-proton interaction. An even more sensitive probe is the so-called $K=0$ odd-even shift (the difference between the observed energy of the 1^- state in a $K=0$ band and the energy of this state calculated by using the rotational formula with parameter values defined by the lowest two even-spin members of the band).

Calculations of parallel-antiparallel splitting energies and odd-even shifts have been made by a number of authors.[38-40] However, until recently[41] theoretical calculations involving a single set of parameters were incapable of calculating successfully both the observed splitting energies and the odd-even shifts for odd-odd deformed nuclei.

We have used the most successful parameter set of Ref. 41 (theory D) to calculate the splittings for ^{188}Re and ^{186}Re. In this formulation the Bartlett, Majorana, Heisenberg, and tensor forces are −63.0, −1.4, 16.0, and −79.2 MeV, respectively, for the finite nuclear range $r_0 = 1.4$ fm. As in the previous comparison between experiment and theory,[41] the Majorana force is not important for these calculations, but the tensor force is particularly important in explaining the odd-even shift.

The calculated results are compared with experiment in Table XIII. It should be noted that the zero-point rotational energies have been subtracted from the band-head energies, using the rotational moment of inertia of that band if it is available or, if not, that of the companion band. The calculated results are in excellent agreement with experiment. We find this agreement particularly impressive in view of the fact that the parametrization used in theory D (Ref. 41) was formulated to fit other data and is entirely independent of the present comparison.

ACKNOWLEDGMENTS

We wish to thank Dr. M. E. Bunker for many invaluable discussions which occurred throughout the course of this work. A valuable contribution was also made by Dr. D. W. Hafemeister, who assisted in the initial phase of this investigation. We are grateful to Dr. H. Motz, Professor H. Maier-Leibnitz, and Professor O. Kofoed-Hansen for their interest in and support of this work. This study involved the use of two reactors and a Van de Graaff accelerator; the authors are indebted to the many people at these facilities who assisted in their operation and in the processing of the data.

†Work supported by the U. S. and Danish Atomic Energy Commissions.

[1] S. B. Burson, E. B. Shera, T. Gedayloo, R. G. Helmer, and D. Zei, Phys. Rev. 136, B1 (1964).

[2] K. Takahashi, M. McKeown, and G. Scharff-Goldhaber, Phys. Rev. 136, B18 (1964).

[3] O. W. B. Schult, B. Weckermann, T. von Egidy, and E. Bieber, Z. Naturforsch. 18a, 61 (1963).

[4] A. M. Berestovoi, I. A. Kondurov, and Yu. E. Loginov, Izv. Akad. Nauk SSSR, Ser. Fiz. 30, 309 (1966) [transl.: Bull. Acad. Sci. USSR, Phys. Ser. 30, 215 (1966)].

[5] P. T. Prokof'ev and L. I. Simonova, Yadern. Fiz. 5, 697 (1967) [transl.: Soviet J. Nucl. Phys. 5, 493 (1967)].

[6] A. A. Suarez, T. von Egidy, W. Kaiser, and H. F.

Mahlein, Nucl. Phys. A107, 417 (1968).
[7]E. T. Jurney, H. T. Motz, and S. H. Vegors, Jr., Nucl. Phys. A94, 351 (1967).
[8]R. C. Greenwood, Phys. Letters 27B, 275 (1968).
[9]G. E. Thomas, D. E. Blatchley, and L. M. Bollinger, Nucl. Instr. Methods 56, 325 (1967).
[10]M. G. Strauss, F. R. Lenkszus, and J. J. Eichholz, Nucl. Instr. Methods 52, 285 (1969).
[11]*Neutron Cross Sections*, compiled by M. D. Goldberg, S. F. Mughabghab, S. N. Purohit, B. A. Magurno, and V. M. May, BNL Report No. BNL-325 (U. S. GPO, Washington, D. C., 1966), 2nd ed., Suppl. 2, Vol. IIC.
[12]R. G. Lanier, R. K. Sheline, H. F. Mahlein, T. von Egidy, W. Kaiser, H. R. Koch, U. Gruber, B. P. K. Maier, O. W. B. Schult, D. W. Hafemeister, and E. B. Shera, Phys. Rev. 178, 1919 (1969).
[13]U. Gruber, B. P. Maier, and O. W. B. Schult, Kerntechnik 5, 17 (1963); B. P. Maier, U. Gruber, and O. W. B. Schult, *ibid.* 5, 19 (1963).
[14]O. W. B. Schult, U. Gruber, B. P. Maier, and F. Stanek, Z. Physik 180, 298 (1964).
[15]The enriched target was obtained from Separated Isotopes Division, Union Carbide Corporation, Oak Ridge, Tennessee 37831.
[16]P. Bergvall, Arkiv Fysik 16, 57 (1960).
[17]E. B. Shera and D. W. Hafemeister, Phys. Rev. 150, 894 (1966); E. B. Shera and H. H. Bolotin, *ibid.* 169, 940 (1968).
[18]Supported by the U. S. Atomic Energy Commission and the Nuclear Program of the State of Florida and by the U. S. Office of Scientific Research under Contract No. AF OSR-62-423.
[19]C. P. Browne and W. W. Buechner, Rev. Sci. Instr. 27, 899 (1956).
[20]For more details of the experimental procedure refer to: M. M. Vergnes and R. K. Sheline, Phys. Rev. 132, 1736 (1963); R. A. Kenefick and R. K. Sheline, *ibid.* 133, B11 (1964); and W. N. Shelton and R. K. Sheline, *ibid.* 133, B624 (1964).
[21]K. E. Chellis and R. K. Sheline, Nucl. Instr. Methods 54, 139 (1967).
[22]We are indebted to H. Kaufmann for making a version of his program, STRIP, available to us.
[23]W. F. Hildebrand and G. E. F. Lundell, *Applied Inorganic Analysis* (Wiley, New York, 1953).
[24]W. M. Doyle and R. Marrus, Nucl. Phys. 49, 449 1963).
[25]J. A. Mihelich, Phys. Rev. 89, 407A (1953).
[26]A. Flammersfeld, Z. Naturforsch. 89, 217 (1953).
[27]K. E. G. Löbner, M. Vetter, and V. Hönig, Nucl. Data A7, 495 (1970).
[28]L. Armstrong and R. Marrus, Phys. Rev. 138, B310 (1965).
[29]M. E. Bunker and C. W. Reich, Rev. Mod. Phys. 43, 348 (1971).
[30]C. J. Gallagher, Jr., and S. A. Moszkowski, Phys. Rev. 111, 1282 (1958).
[31]K. E. G. Löbner, Phys. Letters 26B, 369 (1968).
[32]G. Alaga, Nucl. Phys. 4, 625 (1957).
[33]J. Damgaard, Nucl. Phys. 79, 274 (1966).
[34]M. H. MacFarlane and J. B. French, Rev. Mod. Phys. 32, 567 (1960).
[35]P. D. Kunz and E. Rost, University of Colorado, Boulder, Colorado 80302, private communication.
[36]R. H. Siemssen and J. R. Erskine, Phys. Rev. 146, 911 (1966).
[37]A. Faessler and R. K. Sheline, Phys. Rev. 148, 1003 (1966).
[38]N. D. Newby, Phys. Rev. 125, 2063 (1962).
[39]N. I. Pyatov, Izv. Akad. Nauk SSSR, Ser. Fiz. 27, 1436 (1963) [transl.: Bull. Acad. Sci. USSR, Phys. Ser. 27, 1409 (1963)].
[40]A. G. DePinho and J. Piccard, Nucl. Phys. 65, 426 (1965).
[41]H. D. Jones, N. Onishi, T. Hess, and R. K. Sheline, Phys. Rev. C 3, 529 (1971).